Theoretical status of $\bar{B} \to X_s\gamma$ and $\bar{B} \to X_s\ell^+\ell^-$

Mikołaj Misiak
University of Warsaw

CKM 2018, September 17th-21st 2018, Heidelberg

1. Introduction
2. The isospin asymmetry in $\bar{B} \to X_s\gamma$
3. Resolved photons in $\bar{B} \to X_s\gamma$ and $\bar{B} \to X_s\ell^+\ell^-$
4. Cuts in q^2 and M_{X_s}
5. Status of the perturbative calculations
6. Summary

The most important operators for $\bar{B} \to X_s \gamma$ and $\bar{B} \to X_s \ell^+ \ell^-$:

$$Q_7 = \frac{e m_b}{16\pi^2} \bar{s}_L \sigma_{\mu\nu} b_R F^{\mu\nu} \qquad Q_{9(10)}^{(\ell)} = \frac{e^2}{16\pi^2} [\bar{s}_L \gamma^\alpha b_L] [\bar{\ell} \gamma_\alpha (\gamma_5) \ell]$$

The most important operators for $\bar{B} \to X_s \gamma$ and $\bar{B} \to X_s \ell^+ \ell^-$:

$$Q_7 = \frac{e m_b}{16\pi^2} \bar{s}_L \sigma_{\mu\nu} b_R F^{\mu\nu} \qquad\qquad Q_{9(10)}^{(\ell)} = \frac{e^2}{16\pi^2} \left[\bar{s}_L \gamma^\alpha b_L\right] \left[\bar{\ell} \gamma_\alpha (\gamma_5) \ell\right]$$

Loops from 4-quark operators: 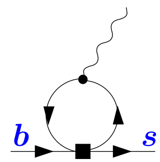

$\to C_7^{\text{eff}}$, 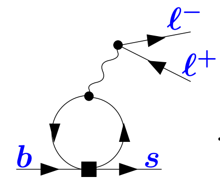

$\to C_9^{(\ell)\text{eff}}(q^2)$.

The most important operators for $\bar{B} \to X_s \gamma$ and $\bar{B} \to X_s \ell^+ \ell^-$:

$$Q_7 = \frac{e m_b}{16\pi^2} \bar{s}_L \sigma_{\mu\nu} b_R F^{\mu\nu} \qquad\qquad Q_{9(10)}^{(\ell)} = \frac{e^2}{16\pi^2} \left[\bar{s}_L \gamma^\alpha b_L\right] \left[\bar{\ell} \gamma_\alpha (\gamma_5) \ell\right]$$

Loops from 4-quark operators: 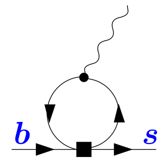

$\to C_7^{\text{eff}}$, 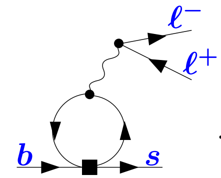

$\to C_9^{(\ell)\text{eff}}(q^2)$.

$\left[R_K, R_{K^*}, P_5', \ldots \text{ in } B \to K^{(*)} \ell^+ \ell^-\right]$ can be explained, e.g., by $C_9^{(\mu)\text{NP}} = -C_{10}^{(\mu)\text{NP}} = (-0.67 \pm 0.16)$.

talk by David Straub on Monday

In such a case, $C_{10}^{(\mu)} / C_{10}^{(\mu)\text{SM}} = 0.84 \pm 0.04$

The most important operators for $\bar{B} \to X_s \gamma$ and $\bar{B} \to X_s \ell^+ \ell^-$:

$$Q_7 = \frac{e m_b}{16\pi^2} \bar{s}_L \sigma_{\mu\nu} b_R F^{\mu\nu} \qquad\qquad Q_{9(10)}^{(\ell)} = \frac{e^2}{16\pi^2} \left[\bar{s}_L \gamma^\alpha b_L\right] \left[\bar{\ell} \gamma_\alpha (\gamma_5) \ell\right]$$

Loops from 4-quark operators:

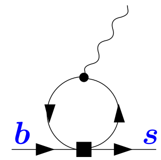

$\to C_7^{\text{eff}}$,

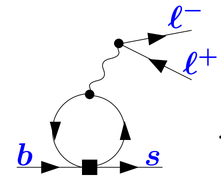

$\to C_9^{(\ell)\text{eff}}(q^2)$.

$\left[R_K, R_{K^*}, P_5', \ldots \text{ in } B \to K^{(*)} \ell^+ \ell^-\right]$ can be explained, e.g., by $C_9^{(\mu)\text{NP}} = -C_{10}^{(\mu)\text{NP}} = (-0.67 \pm 0.16)$.

talk by David Straub on Monday

In such a case, $C_{10}^{(\mu)} / C_{10}^{(\mu)\text{SM}} = 0.84 \pm 0.04$

Alternatively, with $\left|C_{10}^{(\mu)}\right|$ from $B_s \to \mu^+ \mu^-$ alone, and $|C_7|$ from $\bar{B} \to X_s \gamma$, we can extract $C_9^{(\mu)}$ from inclusive $\bar{B} \to X_s \mu^+ \mu^-$ observables: $(H_T, H_L, H_A) \Leftrightarrow (\mathcal{B}, A_{\text{FB}}, \ldots)$.

The most important operators for $\bar{B} \to X_s \gamma$ and $\bar{B} \to X_s \ell^+ \ell^-$:

$$Q_7 = \frac{e m_b}{16\pi^2} \bar{s}_L \sigma_{\mu\nu} b_R F^{\mu\nu} \qquad Q_{9(10)}^{(\ell)} = \frac{e^2}{16\pi^2} \left[\bar{s}_L \gamma^\alpha b_L\right] \left[\bar{\ell} \gamma_\alpha (\gamma_5) \ell\right]$$

Loops from 4-quark operators:

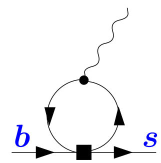

$\to C_7^{\text{eff}}$,

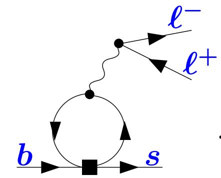

$\to C_9^{(\ell)\text{eff}}(q^2)$.

$\left[R_K, R_{K^*}, P_5', \ldots \text{ in } B \to K^{(*)}\ell^+\ell^-\right]$ can be explained, e.g., by $C_9^{(\mu)\text{NP}} = -C_{10}^{(\mu)\text{NP}} = (-0.67 \pm 0.16)$.

talk by David Straub on Monday

In such a case, $C_{10}^{(\mu)} / C_{10}^{(\mu)\text{SM}} = 0.84 \pm 0.04$

Alternatively, with $\left|C_{10}^{(\mu)}\right|$ from $B_s \to \mu^+\mu^-$ alone, and $|C_7|$ from $\bar{B} \to X_s \gamma$, we can extract $C_9^{(\mu)}$ from inclusive $\bar{B} \to X_s \mu^+ \mu^-$ observables: $(H_T, H_L, H_A) \Leftrightarrow (\mathcal{B}, A_{\text{FB}}, \ldots)$.

$$\frac{d^2\Gamma}{dq^2\,dz} = \frac{3}{8}\left[(1+z^2) H_T(q^2) + 2(1-z^2) H_L(q^2) + 2z H_A(q^2)\right], \quad \begin{array}{l} z = \cos\left[\sphericalangle(\vec{p}_{\ell^+}, \vec{p}_B)\right] \\ \text{in the dilepton frame} \end{array}$$

The most important operators for $\bar{B} \to X_s \gamma$ and $\bar{B} \to X_s \ell^+ \ell^-$:

$$Q_7 = \frac{e m_b}{16\pi^2} \bar{s}_L \sigma_{\mu\nu} b_R F^{\mu\nu} \qquad Q_{9(10)}^{(\ell)} = \frac{e^2}{16\pi^2} \left[\bar{s}_L \gamma^\alpha b_L\right] \left[\bar{\ell} \gamma_\alpha (\gamma_5) \ell\right]$$

Loops from 4-quark operators: 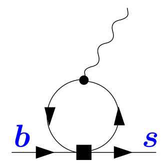

$\to C_7^{\rm eff}$, 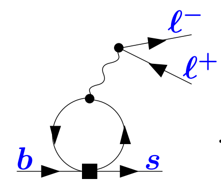

$\to C_9^{(\ell){\rm eff}}(q^2)$.

$\left[R_K, R_{K^*}, P_5', \ldots \text{ in } B \to K^{(*)} \ell^+ \ell^-\right]$ can be explained, e.g., by $C_9^{(\mu){\rm NP}} = -C_{10}^{(\mu){\rm NP}} = (-0.67 \pm 0.16)$.

talk by David Straub on Monday

In such a case, $C_{10}^{(\mu)} / C_{10}^{(\mu){\rm SM}} = 0.84 \pm 0.04$

Alternatively, with $\left|C_{10}^{(\mu)}\right|$ from $B_s \to \mu^+ \mu^-$ alone, and $\left|C_7\right|$ from $\bar{B} \to X_s \gamma$, we can extract $C_9^{(\mu)}$ from inclusive $\bar{B} \to X_s \mu^+ \mu^-$ observables: $(H_T, H_L, H_A) \Leftrightarrow (\mathcal{B}, A_{\rm FB}, \ldots)$.

$$\frac{d^2\Gamma}{dq^2\, dz} = \frac{3}{8} \left[(1+z^2) H_T(q^2) + 2(1-z^2) H_L(q^2) + 2z H_A(q^2)\right],$$

$z = \cos\left[\sphericalangle(\vec{p}_{\ell^+}, \vec{p}_B)\right]$ in the dilepton frame

$\left|C_{10}^{(\mu)}\right|$ from the average time-integrated $B_s \to \mu^+ \mu^-$ branching ratio:

$$\overline{\mathcal{B}}_{s\mu}^{\rm exp} \times 10^9 = 2.93 \underbrace{\pm 0.46}_{\pm 16\%}$$

naive average of LHCb, arXiv:1703.05747, CMS, arXiv:1307.5025 ATLAS, talk by Alex Cerri today

$$\overline{\mathcal{B}}_{s\mu}^{\rm SM} \times 10^9 = 3.54 \underbrace{\pm 0.21}_{\pm 6\%}$$

arXiv:1311.0903 with updates in arXiv:1803.10097

$$\Rightarrow \left| \frac{C_{10}^{(\mu)}}{C_{10}^{(\mu){\rm SM}}} \right| = 0.91 \pm 0.08 \;\; (1.1\sigma)$$

The most important operators for $\bar{B} \to X_s \gamma$ and $\bar{B} \to X_s \ell^+ \ell^-$:

$$Q_7 = \frac{e m_b}{16\pi^2} \bar{s}_L \sigma_{\mu\nu} b_R F^{\mu\nu} \qquad Q_{9(10)}^{(\ell)} = \frac{e^2}{16\pi^2} \left[\bar{s}_L \gamma^\alpha b_L\right] \left[\bar{\ell}\gamma_\alpha(\gamma_5)\ell\right]$$

Loops from 4-quark operators: 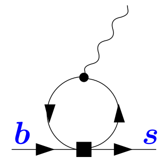 $\to C_7^{\text{eff}}$, 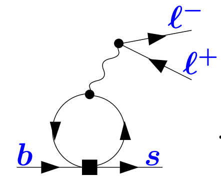 $\to C_9^{(\ell)\text{eff}}(q^2)$.

$\left[R_K, R_{K^*}, P_5', \ldots \text{ in } B \to K^{(*)}\ell^+\ell^-\right]$ can be explained, e.g., by $C_9^{(\mu)\text{NP}} = -C_{10}^{(\mu)\text{NP}} = (-0.67 \pm 0.16)$.

talk by David Straub on Monday

In such a case, $C_{10}^{(\mu)} / C_{10}^{(\mu)\text{SM}} = 0.84 \pm 0.04$

Alternatively, with $|C_{10}^{(\mu)}|$ from $B_s \to \mu^+\mu^-$ alone, and $|C_7|$ from $\bar{B} \to X_s \gamma$, we can extract $C_9^{(\mu)}$ from inclusive $\bar{B} \to X_s \mu^+\mu^-$ observables: $(H_T, H_L, H_A) \Leftrightarrow (\mathcal{B}, A_{\text{FB}}, \ldots)$.

$$\frac{d^2\Gamma}{dq^2\, dz} = \frac{3}{8}\left[(1+z^2)H_T(q^2) + 2(1-z^2)H_L(q^2) + 2zH_A(q^2)\right],$$

$z = \cos\left[\sphericalangle(\vec{p}_{\ell^+}, \vec{p}_B)\right]$ in the dilepton frame

$|C_{10}^{(\mu)}|$ from the average time-integrated $B_s \to \mu^+\mu^-$ branching ratio:

$$\overline{\mathcal{B}}_{s\mu}^{\text{exp}} \times 10^9 = 2.93 \underbrace{\pm 0.46}_{\pm 16\%}$$

naive average of LHCb, arXiv:1703.05747, CMS, arXiv:1307.5025 ATLAS, talk by Alex Cerri today

$$\overline{\mathcal{B}}_{s\mu}^{\text{SM}} \times 10^9 = 3.54 \underbrace{\pm 0.21}_{\pm 6\%}$$

arXiv:1311.0903 with updates in arXiv:1803.10097

$$\Rightarrow \left|\frac{C_{10}^{(\mu)}}{C_{10}^{(\mu)\text{SM}}}\right| = 0.91 \pm 0.08 \;\; (1.1\sigma)$$

The same central values would give $> 2\sigma$ with the future $\pm 6\%$ in $\overline{\mathcal{B}}_{s\mu}^{\text{exp}}$ [LHCb].

$|C_7|$ **from the CP- and isospin-averaged branching ratio of** $\bar{B} \to X_s\gamma$ **with** $E_\gamma > 1.6\,\mathrm{GeV}$:

$$\mathcal{B}^{\mathrm{exp}}_{s\gamma} \times 10^4 = 3.32 \underbrace{\pm 0.15}_{\pm 4.5\%}$$

HFLAV, arXiv:1612.07233, average of Belle, BaBar and CLEO.

$$\mathcal{B}^{\mathrm{SM}}_{s\gamma} \times 10^4 = 3.36 \underbrace{\pm 0.23}_{\pm 6.9\%}$$

arXiv:1503.01789, arXiv:1503.01791.

$$\Rightarrow \frac{C_7(\mu_b)}{C_7^{\mathrm{SM}}(\mu_b)} = 0.99 \pm 0.07$$

$|C_7|$ **from the CP- and isospin-averaged branching ratio of** $\bar{B} \to X_s\gamma$ **with** $E_\gamma > 1.6\,\mathrm{GeV}$:

$$\left.\begin{array}{ll} \mathcal{B}_{s\gamma}^{\mathrm{exp}} \times 10^4 = 3.32 \underbrace{\pm 0.15}_{\pm 4.5\%} & \text{HFLAV, arXiv:1612.07233, average of Belle, BaBar and CLEO.} \\ \mathcal{B}_{s\gamma}^{\mathrm{SM}} \times 10^4 = 3.36 \underbrace{\pm 0.23}_{\pm 6.9\%} & \text{arXiv:1503.01789, arXiv:1503.01791.} \end{array}\right\} \Rightarrow \frac{C_7(\mu_b)}{C_7^{\mathrm{SM}}(\mu_b)} = 0.99 \pm 0.07$$

Belle II with $50\,\mathrm{ab}^{-1}$ **is going to reach** $\pm 2.3\%$ **in** $\mathcal{B}_{s\gamma}^{\mathrm{exp}}$ [naive weighted average of $\pm 3.2\%$, $\pm 4.2\%$ and $\pm 5.7\%$ obtained for $E_\gamma > 1.9\,\mathrm{GeV}$ using different methods in Table 61 of The Belle II Physics Book, arXiv:1808.10567.]

$|C_7|$ **from the CP- and isospin-averaged branching ratio of** $\bar{B} \to X_s \gamma$ **with** $E_\gamma > 1.6\,\text{GeV}$:

$$\left.\begin{array}{l} \mathcal{B}^{\text{exp}}_{s\gamma} \times 10^4 = 3.32 \underbrace{\pm 0.15}_{\pm 4.5\%} \quad \text{HFLAV, arXiv:1612.07233, average of Belle, BaBar and CLEO.} \\ \mathcal{B}^{\text{SM}}_{s\gamma} \times 10^4 = 3.36 \underbrace{\pm 0.23}_{\pm 6.9\%} \quad \text{arXiv:1503.01789, arXiv:1503.01791.} \end{array}\right\} \Rightarrow \frac{C_7(\mu_b)}{C_7^{\text{SM}}(\mu_b)} = 0.99 \pm 0.07$$

Belle II with $50\,\text{ab}^{-1}$ **is going to reach** $\pm 2.3\%$ **in** $\mathcal{B}^{\text{exp}}_{s\gamma}$ [naive weighted average of $\pm 3.2\%$, $\pm 4.2\%$ and $\pm 5.7\%$ obtained for $E_\gamma > 1.9\,\text{GeV}$ using different methods in Table 61 of The Belle II Physics Book, arXiv:1808.10567.]

Thus, the TH uncertainty must be reduced.
At present, it consists of four contributions (summed in quadrature):

5% **non-perturbative,** **3%** **from the interpolation in** m_c,
3% **higher order** $\mathcal{O}(\alpha_s^3)$, **2%** **parametric.**

$|C_7|$ from the CP- and isospin-averaged branching ratio of $\bar{B} \to X_s\gamma$ with $E_\gamma > 1.6\,\mathrm{GeV}$:

$$\mathcal{B}_{s\gamma}^{\rm exp} \times 10^4 = 3.32 \underbrace{\pm\, 0.15}_{\pm 4.5\%}$$

HFLAV, arXiv:1612.07233, average of Belle, BaBar and CLEO.

$$\mathcal{B}_{s\gamma}^{\rm SM} \times 10^4 = 3.36 \underbrace{\pm\, 0.23}_{\pm 6.9\%}$$

arXiv:1503.01789, arXiv:1503.01791.

$$\Rightarrow \frac{C_7(\mu_b)}{C_7^{\rm SM}(\mu_b)} = 0.99 \pm 0.07$$

Belle II with $50\,\mathrm{ab}^{-1}$ is going to reach $\pm 2.3\%$ in $\mathcal{B}_{s\gamma}^{\rm exp}$

[naive weighted average of $\pm 3.2\%$, $\pm 4.2\%$ and $\pm 5.7\%$ obtained for $E_\gamma > 1.9\,\mathrm{GeV}$ using different methods in Table 61 of The Belle II Physics Book, arXiv:1808.10567.]

Thus, the TH uncertainty must be reduced.
At present, it consists of four contributions (summed in quadrature):

5% non-perturbative, 3% from the interpolation in m_c,
3% higher order $\mathcal{O}(\alpha_s^3)$, 2% parametric.

Effect of the interpolated $\mathcal{O}(\alpha_s^2)$ contribution on the branching ratio:

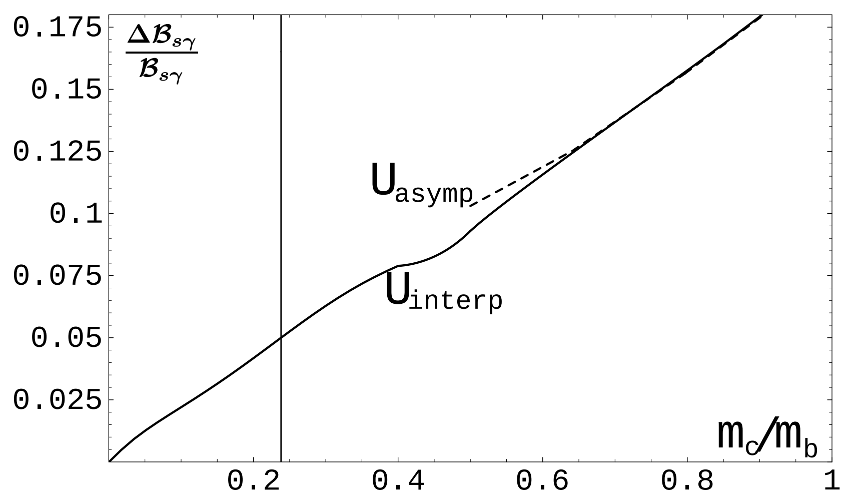

The $\pm 5\%$ non-perturbative uncertainty is practically saturated by the so-called resolved photon contributions whose effects have been estimated in the SCET analysis of Benzke, Lee, Neubert, Paz, arXiv:1003.5012:

The $\pm 5\%$ non-perturbative uncertainty is practically saturated by the so-called resolved photon contributions whose effects have been estimated in the SCET analysis of
Benzke, Lee, Neubert, Paz, arXiv:1003.5012:

interference	ranges		"TH 1σ"	
	original	at present	original	at present
Q_7–Q_8	$[-2.8, -0.3]\%$	$[-0.6, 0.9]\%$	$(-1.55 \pm 1.25)\%$	$(0.16 \pm 0.74)\%$
Q_8–Q_8	$[-0.3, 1.9]\%$	no change	$(0.80 \pm 1.10)\%$	no change
Q_7–$Q_{1,2}$	$[-1.7, 4.0]\%$	no change	$(1.15 \pm 2.85)\%$	no change
tot. linear	$[-4.8, 5.6]\%$	$[-2.6, 6.8]\%$	$(0.4 \pm 5.2)\%$	$(2.1 \pm 4.7)\%$
tot. quadrature	$[-2.9, 3.7]\%$	$[-1.1, 5.3]\%$	$(0.4 \pm 3.3)\%$	$(2.1 \pm 3.2)\%$

$\Leftarrow$ Belle Δ_{0-}
arXiv:1807.04236v4

In the 2015 phenomenological update [arXiv:1503.01789, arXiv:1503.01791], $(0 \pm 5\%)$ has been used, and combined in quadrature with other uncertainties.

The $\pm 5\%$ non-perturbative uncertainty is practically saturated by the so-called resolved photon contributions whose effects have been estimated in the SCET analysis of
Benzke, Lee, Neubert, Paz, arXiv:1003.5012:

interference	ranges		"TH 1σ"	
	original	at present	original	at present
Q_7–Q_8	$[-2.8, -0.3]\%$	$[-0.6, 0.9]\%$	$(-1.55 \pm 1.25)\%$	$(0.16 \pm 0.74)\%$
Q_8–Q_8	$[-0.3, 1.9]\%$	no change	$(0.80 \pm 1.10)\%$	no change
Q_7–$Q_{1,2}$	$[-1.7, 4.0]\%$	no change	$(1.15 \pm 2.85)\%$	no change
tot. linear	$[-4.8, 5.6]\%$	$[-2.6, 6.8]\%$	$(0.4 \pm 5.2)\%$	$(2.1 \pm 4.7)\%$
tot. quadrature	$[-2.9, 3.7]\%$	$[-1.1, 5.3]\%$	$(0.4 \pm 3.3)\%$	$(2.1 \pm 3.2)\%$

$\Leftarrow$ Belle Δ_{0-}
arXiv:1807.04236v4

In the 2015 phenomenological update [arXiv:1503.01789, arXiv:1503.01791], $(0 \pm 5\%)$ has been used, and combined in quadrature with other uncertainties.

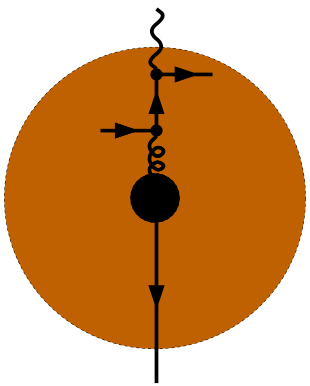

The resolved photon contribution to the Q_7–Q_8 interference originates from hard gluon scattering on the valence quark or a "sea" quark that produces an energetic photon. The quark that undergoes this Compton-like scattering is assumed to remain soft in the $\bar{B}$-meson rest frame to ensure effective interference with the leading "hard" amplitude. Without interference the contribution would be negligible $(\mathcal{O}(\alpha_s^2 \Lambda^2 / m_b^2))$.

Suppression by Λ can be understood as originating from dilution of the target (size of the $\bar{B}$-meson $\sim \Lambda^{-1}$).

The $\pm5\%$ non-perturbative uncertainty is practically saturated by the so-called resolved photon contributions whose effects have been estimated in the SCET analysis of
Benzke, Lee, Neubert, Paz, arXiv:1003.5012:

interference	ranges		"TH 1σ"	
	original	at present	original	at present
Q_7–Q_8	$[-2.8, -0.3]\%$	$[-0.6, 0.9]\%$	$(-1.55 \pm 1.25)\%$	$(0.16 \pm 0.74)\%$
Q_8–Q_8	$[-0.3, 1.9]\%$	no change	$(0.80 \pm 1.10)\%$	no change
Q_7–$Q_{1,2}$	$[-1.7, 4.0]\%$	no change	$(1.15 \pm 2.85)\%$	no change
tot. linear	$[-4.8, 5.6]\%$	$[-2.6, 6.8]\%$	$(0.4 \pm 5.2)\%$	$(2.1 \pm 4.7)\%$
tot. quadrature	$[-2.9, 3.7]\%$	$[-1.1, 5.3]\%$	$(0.4 \pm 3.3)\%$	$(2.1 \pm 3.2)\%$

$\Leftarrow$ Belle Δ_{0-}
arXiv:1807.04236v4

In the 2015 phenomenological update [arXiv:1503.01789, arXiv:1503.01791], $(0 \pm 5\%)$ has been used, and combined in quadrature with other uncertainties.

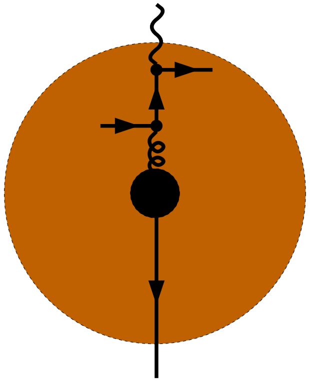

The resolved photon contribution to the Q_7–Q_8 interference originates from hard gluon scattering on the valence quark or a "sea" quark that produces an energetic photon. The quark that undergoes this Compton-like scattering is assumed to remain soft in the $\bar{B}$-meson rest frame to ensure effective interference with the leading "hard" amplitude. Without interference the contribution would be negligible $(\mathcal{O}(\alpha_s^2 \Lambda^2/m_b^2))$.

Suppression by Λ can be understood as originating from dilution of the target (size of the $\bar{B}$-meson $\sim \Lambda^{-1}$).

Dominant in Δ_{0-}: $\quad \Gamma[B^- \to X_s\gamma] \simeq A + BQ_u + CQ_d + DQ_s, \quad \Gamma[\bar{B}^0 \to X_s\gamma] \simeq A + BQ_d + CQ_u + DQ_s$

The $\pm 5\%$ non-perturbative uncertainty is practically saturated by the so-called resolved photon contributions whose effects have been estimated in the SCET analysis of Benzke, Lee, Neubert, Paz, arXiv:1003.5012:

interference	ranges		"TH 1σ"	
	original	at present	original	at present
Q_7–Q_8	$[-2.8, -0.3]\%$	$[-0.6, 0.9]\%$	$(-1.55 \pm 1.25)\%$	$(0.16 \pm 0.74)\%$
Q_8–Q_8	$[-0.3, 1.9]\%$	no change	$(0.80 \pm 1.10)\%$	no change
Q_7–$Q_{1,2}$	$[-1.7, 4.0]\%$	no change	$(1.15 \pm 2.85)\%$	no change
tot. linear	$[-4.8, 5.6]\%$	$[-2.6, 6.8]\%$	$(0.4 \pm 5.2)\%$	$(2.1 \pm 4.7)\%$
tot. quadrature	$[-2.9, 3.7]\%$	$[-1.1, 5.3]\%$	$(0.4 \pm 3.3)\%$	$(2.1 \pm 3.2)\%$

$\Leftarrow$ Belle Δ_{0-} arXiv:1807.04236v4

In the 2015 phenomenological update [arXiv:1503.01789, arXiv:1503.01791], $(0 \pm 5\%)$ has been used, and combined in quadrature with other uncertainties.

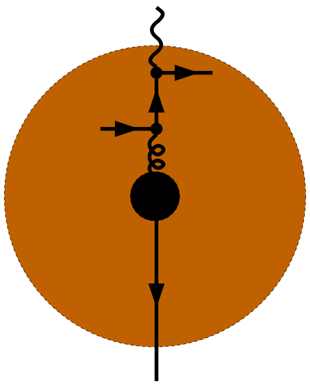

The resolved photon contribution to the Q_7–Q_8 interference originates from hard gluon scattering on the valence quark or a "sea" quark that produces an energetic photon. The quark that undergoes this Compton-like scattering is assumed to remain soft in the $\bar{B}$-meson rest frame to ensure effective interference with the leading "hard" amplitude. Without interference the contribution would be negligible ($\mathcal{O}(\alpha_s^2 \Lambda^2/m_b^2)$).

Suppression by Λ can be understood as originating from dilution of the target (size of the $\bar{B}$-meson $\sim \Lambda^{-1}$).

Dominant in Δ_{0-}: $\quad \Gamma[B^- \to X_s\gamma] \simeq A + BQ_u + CQ_d + DQ_s, \quad \Gamma[\bar{B}^0 \to X_s\gamma] \simeq A + BQ_d + CQ_u + DQ_s$

Isospin-averaged decay rate: $\quad \Gamma \simeq A + \frac{1}{2}(B+C)(Q_u + Q_d) + DQ_s \equiv A + \delta\Gamma_{78\text{res}}$

Isospin asymmetry: $\quad \Delta_{0-} \simeq \frac{C-B}{2\Gamma}(Q_u - Q_d)$

The $\pm 5\%$ non-perturbative uncertainty is practically saturated by the so-called resolved photon contributions whose effects have been estimated in the SCET analysis of Benzke, Lee, Neubert, Paz, arXiv:1003.5012:

interference	ranges		"TH 1σ"	
	original	at present	original	at present
Q_7–Q_8	$[-2.8, -0.3]\%$	$[-0.6, 0.9]\%$	$(-1.55 \pm 1.25)\%$	$(0.16 \pm 0.74)\%$
Q_8–Q_8	$[-0.3, 1.9]\%$	no change	$(0.80 \pm 1.10)\%$	no change
Q_7–$Q_{1,2}$	$[-1.7, 4.0]\%$	no change	$(1.15 \pm 2.85)\%$	no change
tot. linear	$[-4.8, 5.6]\%$	$[-2.6, 6.8]\%$	$(0.4 \pm 5.2)\%$	$(2.1 \pm 4.7)\%$
tot. quadrature	$[-2.9, 3.7]\%$	$[-1.1, 5.3]\%$	$(0.4 \pm 3.3)\%$	$(2.1 \pm 3.2)\%$

$\Leftarrow$ Belle Δ_{0-} arXiv:1807.04236v4

In the 2015 phenomenological update [arXiv:1503.01789, arXiv:1503.01791], $(0 \pm 5\%)$ has been used, and combined in quadrature with other uncertainties.

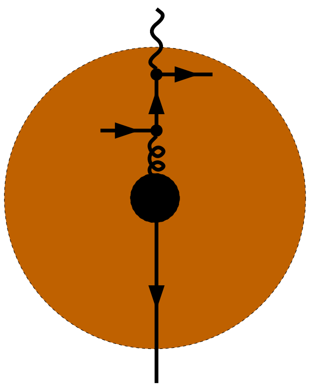

The resolved photon contribution to the Q_7–Q_8 interference originates from hard gluon scattering on the valence quark or a "sea" quark that produces an energetic photon. The quark that undergoes this Compton-like scattering is assumed to remain soft in the $\bar{B}$-meson rest frame to ensure effective interference with the leading "hard" amplitude. Without interference the contribution would be negligible ($\mathcal{O}(\alpha_s^2 \Lambda^2/m_b^2)$).

Suppression by Λ can be understood as originating from dilution of the target (size of the $\bar{B}$-meson $\sim \Lambda^{-1}$).

Dominant in Δ_{0-}: $\quad \Gamma[B^- \to X_s\gamma] \simeq A + BQ_u + CQ_d + DQ_s, \quad \Gamma[\bar{B}^0 \to X_s\gamma] \simeq A + BQ_d + CQ_u + DQ_s$

Isospin-averaged decay rate: $\quad \Gamma \simeq A + \frac{1}{2}(B+C)(Q_u+Q_d) + DQ_s \equiv A + \delta\Gamma_{78\text{res}}$

Isospin asymmetry: $\quad \Delta_{0-} \simeq \frac{C-B}{2\Gamma}(Q_u - Q_d)$

$$\Rightarrow \quad \frac{\delta\Gamma_{78\text{res}}/\Gamma}{\Delta_{0-}} \simeq \frac{(B+C)(Q_u+Q_d)+2DQ_s}{(C-B)(Q_u-Q_d)} = \frac{Q_u+Q_d}{Q_d-Q_u}\left[1 + 2\,\frac{D-C}{C-B}\right]$$

The $\pm 5\%$ non-perturbative uncertainty is practically saturated by the so-called resolved photon contributions whose effects have been estimated in the SCET analysis of
Benzke, Lee, Neubert, Paz, arXiv:1003.5012:

interference	ranges		"TH 1σ"	
	original	at present	original	at present
Q_7–Q_8	$[-2.8, -0.3]\%$	$[-0.6, 0.9]\%$	$(-1.55 \pm 1.25)\%$	$(0.16 \pm 0.74)\%$
Q_8–Q_8	$[-0.3, 1.9]\%$	no change	$(0.80 \pm 1.10)\%$	no change
Q_7–$Q_{1,2}$	$[-1.7, 4.0]\%$	no change	$(1.15 \pm 2.85)\%$	no change
tot. linear	$[-4.8, 5.6]\%$	$[-2.6, 6.8]\%$	$(0.4 \pm 5.2)\%$	$(2.1 \pm 4.7)\%$
tot. quadrature	$[-2.9, 3.7]\%$	$[-1.1, 5.3]\%$	$(0.4 \pm 3.3)\%$	$(2.1 \pm 3.2)\%$

$\Leftarrow$ Belle Δ_{0-}
arXiv:1807.04236v4

In the 2015 phenomenological update [arXiv:1503.01789, arXiv:1503.01791], $(0 \pm 5\%)$ has been used, and combined in quadrature with other uncertainties.

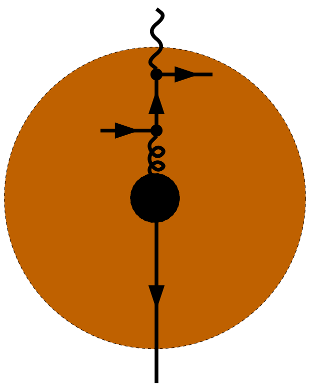

The resolved photon contribution to the Q_7–Q_8 interference originates from hard gluon scattering on the valence quark or a "sea" quark that produces an energetic photon. The quark that undergoes this Compton-like scattering is assumed to remain soft in the $\bar{B}$-meson rest frame to ensure effective interference with the leading "hard" amplitude. Without interference the contribution would be negligible ($\mathcal{O}(\alpha_s^2 \Lambda^2 / m_b^2)$).

Suppression by Λ can be understood as originating from dilution of the target (size of the $\bar{B}$-meson $\sim \Lambda^{-1}$).

Dominant in Δ_{0-}: $\quad \Gamma[B^- \to X_s \gamma] \simeq A + B Q_u + C Q_d + D Q_s, \quad \Gamma[\bar{B}^0 \to X_s \gamma] \simeq A + B Q_d + C Q_u + D Q_s$

Isospin-averaged decay rate: $\quad \Gamma \;\simeq\; A + \frac{1}{2}(B+C)(Q_u + Q_d) + D Q_s \;\equiv\; A + \delta\Gamma_{78\mathrm{res}}$

Isospin asymmetry: $\quad \Delta_{0-} \;\simeq\; \frac{C-B}{2\Gamma}(Q_u - Q_d)$

$$\Rightarrow \quad \frac{\delta\Gamma_{78\mathrm{res}}/\Gamma}{\Delta_{0-}} \;\simeq\; \frac{(B+C)(Q_u+Q_d)+2DQ_s}{(C-B)(Q_u-Q_d)} \;\overset{Q_u+Q_d+Q_s=0}{=}\; \frac{Q_u+Q_d}{Q_d-Q_u}\left[1 + 2\,\overbrace{\frac{D-C}{C-B}}^{SU(3)_F \text{ violation}}\right]$$

MM, arXiv:0911.1651

The $\pm 5\%$ non-perturbative uncertainty is practically saturated by the so-called resolved photon contributions whose effects have been estimated in the SCET analysis of
Benzke, Lee, Neubert, Paz, arXiv:1003.5012:

interference	ranges		"TH 1σ"	
	original	at present	original	at present
Q_7–Q_8	$[-2.8, -0.3]\%$	$[-0.6, 0.9]\%$	$(-1.55 \pm 1.25)\%$	$(0.16 \pm 0.74)\%$
Q_8–Q_8	$[-0.3, 1.9]\%$	no change	$(0.80 \pm 1.10)\%$	no change
Q_7–$Q_{1,2}$	$[-1.7, 4.0]\%$	no change	$(1.15 \pm 2.85)\%$	no change
tot. linear	$[-4.8, 5.6]\%$	$[-2.6, 6.8]\%$	$(0.4 \pm 5.2)\%$	$(2.1 \pm 4.7)\%$
tot. quadrature	$[-2.9, 3.7]\%$	$[-1.1, 5.3]\%$	$(0.4 \pm 3.3)\%$	$(2.1 \pm 3.2)\%$

$\Leftarrow$ Belle Δ_{0-}
arXiv:1807.04236v4

In the 2015 phenomenological update [arXiv:1503.01789, arXiv:1503.01791], $(0 \pm 5\%)$ has been used, and combined in quadrature with other uncertainties.

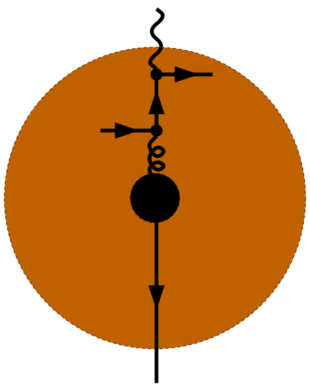

The resolved photon contribution to the Q_7–Q_8 interference originates from hard gluon scattering on the valence quark or a "sea" quark that produces an energetic photon. The quark that undergoes this Compton-like scattering is assumed to remain soft in the $\bar{B}$-meson rest frame to ensure effective interference with the leading "hard" amplitude. Without interference the contribution would be negligible ($\mathcal{O}(\alpha_s^2 \Lambda^2 / m_b^2)$).

Suppression by Λ can be understood as originating from dilution of the target (size of the $\bar{B}$-meson $\sim \Lambda^{-1}$).

Dominant in Δ_{0-}: $\quad \Gamma[B^- \to X_s\gamma] \simeq A + BQ_u + CQ_d + DQ_s, \quad \Gamma[\bar{B}^0 \to X_s\gamma] \simeq A + BQ_d + CQ_u + DQ_s$

Isospin-averaged decay rate: $\quad \Gamma \;\simeq\; A + \frac{1}{2}(B+C)(Q_u+Q_d) + DQ_s \;\equiv\; A + \delta\Gamma_{78\mathrm{res}}$

Isospin asymmetry: $\quad \Delta_{0-} \;\simeq\; \frac{C-B}{2\Gamma}(Q_u - Q_d)$

$$\Rightarrow \quad \frac{\delta\Gamma_{78\mathrm{res}}/\Gamma}{\Delta_{0-}} \;\simeq\; \frac{(B+C)(Q_u+Q_d)+2DQ_s}{(C-B)(Q_u-Q_d)} \;\overset{Q_u+Q_d+Q_s=0}{=}\; \frac{Q_u+Q_d}{Q_d-Q_u}\left[1 + \overbrace{2\,\frac{D-C}{C-B}}^{SU(3)_F \text{ violation}}\right]$$

MM, arXiv:0911.1651

$$\frac{\delta\Gamma_{78\mathrm{res}}}{\Gamma} \simeq -\tfrac{1}{3}\Delta_{0-}\left[1 + 2\,\tfrac{D-C}{C-B}\right] \;=\; -\tfrac{1}{3}(-0.48 \pm 1.49 \pm 0.97 \pm 1.15)\% \times (1 \pm 0.3) \;=\; (0.16 \pm 0.74)\%$$

SM predictions for $\mathcal{B}(\bar{B} \to X_s \ell^+\ell^-) \times 10^6$ with $q^2 \in [1,6]$ GeV and no cut on M_{X_s}:

$$\left.\begin{array}{l} 1.64 \pm 0.11, \;\; \ell = e \\ 1.59 \pm 0.11, \;\; \ell = \mu \end{array}\right\}$$ parametric and perturbative uncert. only [Huber, Lunghi, MM, Wyler, hep-ph/0512066]

$$\left.\begin{array}{l} 1.67 \pm 0.10, \;\; \ell = e \\ 1.62 \pm 0.09, \;\; \ell = \mu \end{array}\right\}$$ param. update + Krüger-Sehgal, [Huber, Hurth, Lunghi, arXiv:1503.04849]

PLB380 (1996) 199
PRD55 (1997) 2799

The corresponding semi-inclusive experimental results:

$$\left.\begin{array}{l} 1.93^{+0.54}_{-0.51}, \;\; \ell = e \\ 0.66^{+0.88}_{-0.80}, \;\; \ell = \mu \end{array}\right\} = 1.60^{+0.48}_{-0.45},$$ Babar, arXiv:1312.5364, $471 \times 10^6 B\bar{B}$, extrapolated from $M_X < 1.8$ GeV.

$1.49^{+0.65}_{-0.58}$, Belle, hep-ex/0503044, $152 \times 10^6 B\bar{B}$.

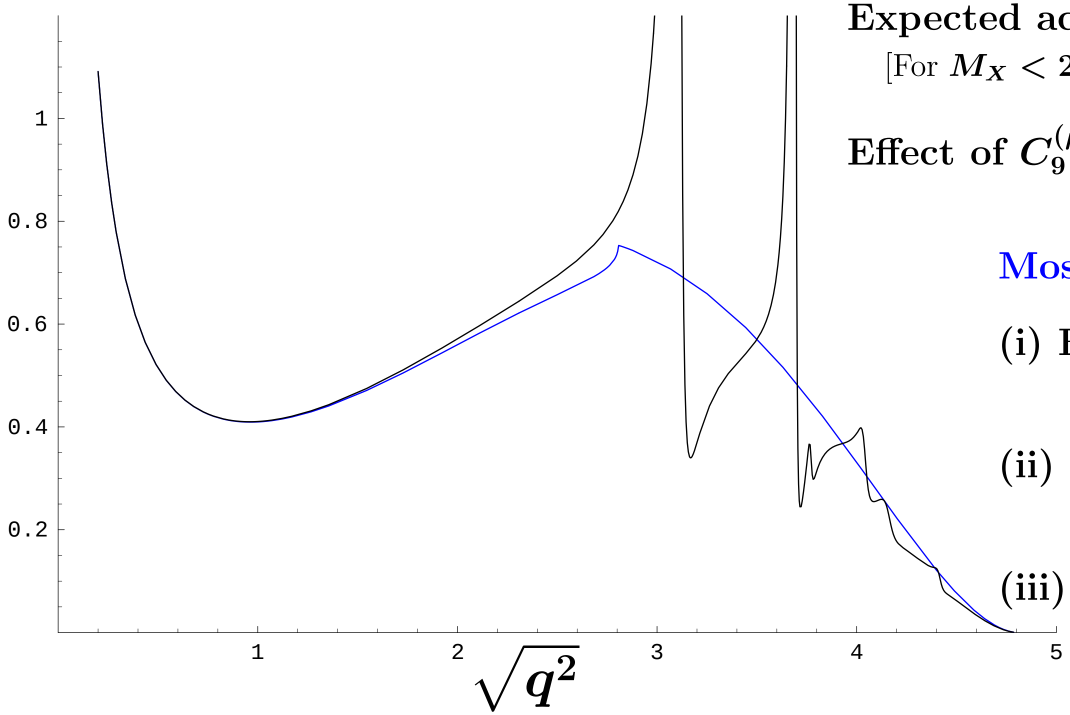

Expected accuracy at Belle II with $50\,\mathrm{ab}^{-1}$: $\sim \pm 6.5\%$.

[For $M_X < 2.0$ GeV, Table 64 of The Belle II Physics Book, arXiv:1808.10567]

Effect of $C_9^{(\mu)\mathrm{NP}} = -C_{10}^{(\mu)\mathrm{NP}} = -0.67$: $\mathcal{B} \searrow \sim 30\%$.

Most recent contributions on the theory side:

(i) Benzke, Hurth, Turczyk, arXiv:1705.10366,
charm loops & resolved photons → next slides.

(ii) de Boer, arXiv:1707.00988,
two loops analytically.

(iii) Huber, Qin, Vos, arXiv:1806.11521,
five body & pheno update → next speaker.
[Qin Qin]

More on resolved photons in $\bar{B} \to X_s\gamma$ and $\bar{B} \to X_s\ell^+\ell^-$

Background-subtracted $\bar{B} \to X_{s+d}\,\gamma$ photon energy spectrum in the $\Upsilon(4S)$ rest frame, from Fig. 1 of the Belle analysis in arXiv:1608.02344.

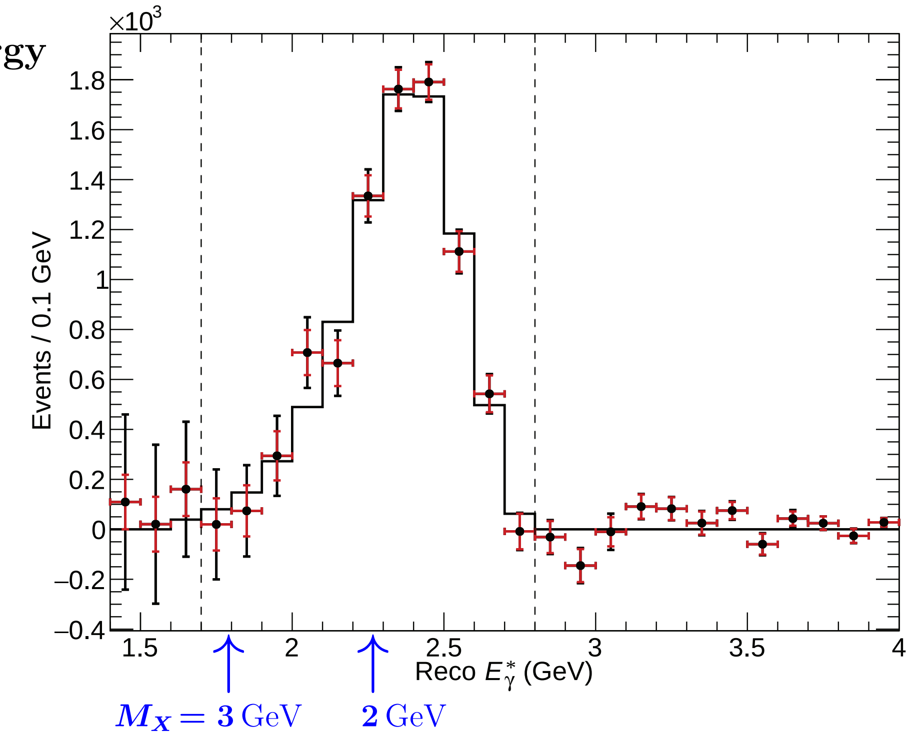

More on resolved photons in $\bar{B} \to X_s\gamma$ and $\bar{B} \to X_s\ell^+\ell^-$

Background-subtracted $\bar{B} \to X_{s+d}\,\gamma$ photon energy spectrum in the $\Upsilon(4S)$ rest frame, from Fig. 1 of the Belle analysis in arXiv:1608.02344.

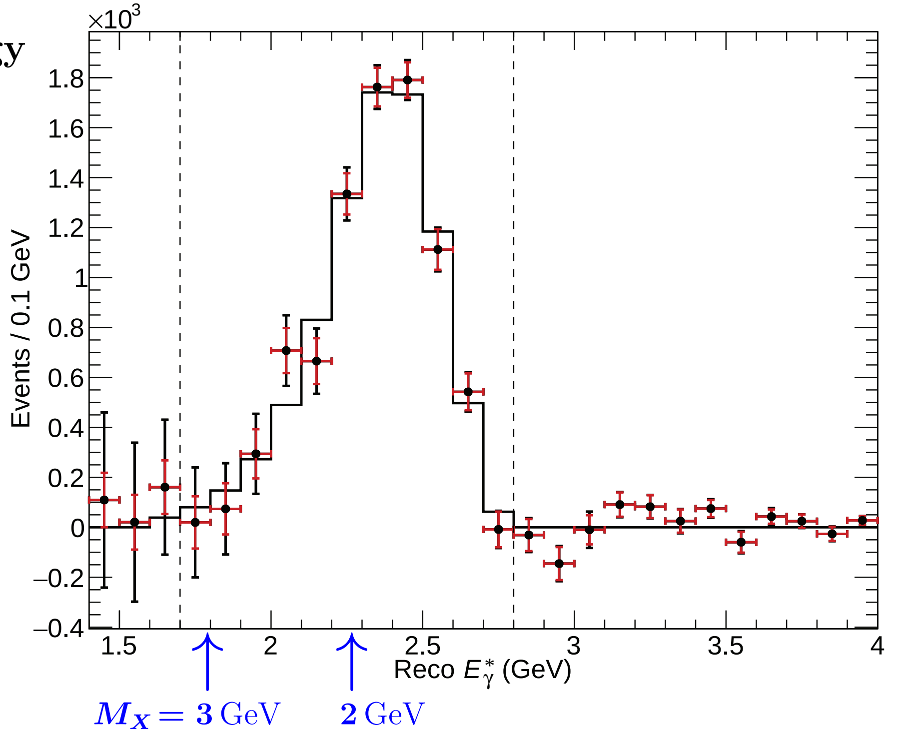

For $M_X \lesssim 3\,\mathrm{GeV}$ and in the absence of 4-quark ops, we have local OPE $\Rightarrow \mathcal{O}(\Lambda^2/m_b^2)$.

More on resolved photons in $\bar{B} \to X_s\gamma$ and $\bar{B} \to X_s\ell^+\ell^-$

Background-subtracted $\bar{B} \to X_{s+d}\,\gamma$ photon energy spectrum in the $\Upsilon(4S)$ rest frame, from Fig. 1 of the Belle analysis in arXiv:1608.02344.

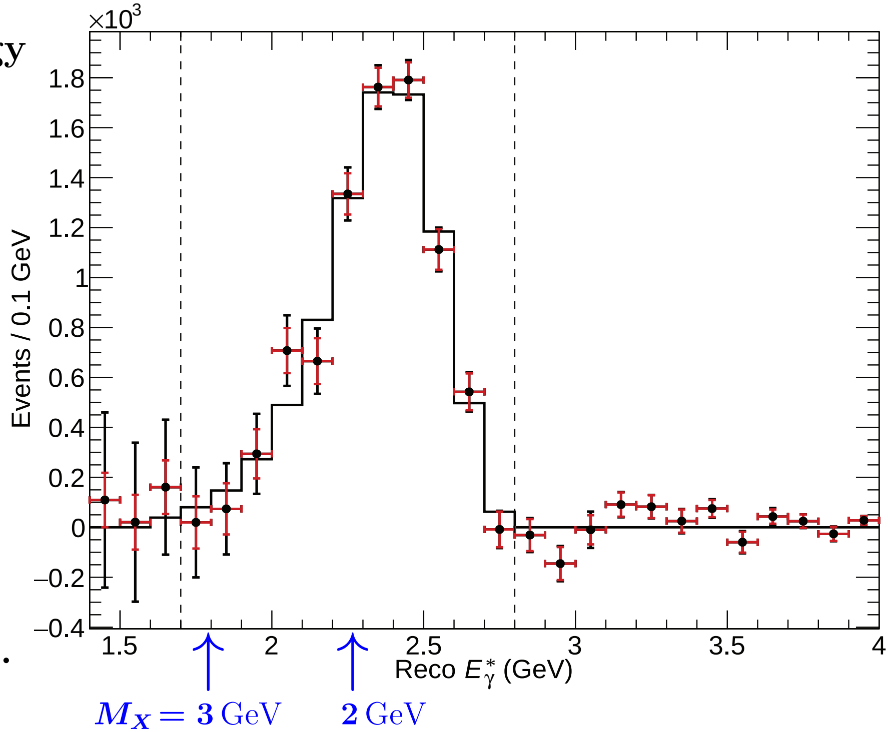

For $M_X \lesssim 3\,\text{GeV}$ and in the absence of 4-quark ops, we have local OPE $\Rightarrow \mathcal{O}(\Lambda^2/m_b^2)$.

In the presence of 4-quark ops:
Light quark loops – suppressed by $C_{3,\dots,6}$ or CKM;
Charm loops – factorizable or local if m_c^2 is sufficiently large w.r.t. $m_b\Lambda$. Numerically, $\mathcal{O}(3\%)$ non-fact. effects found in $\mathcal{B}(\bar{B} \to X_s\gamma)$ and $\mathcal{B}(\bar{B} \to X_s\ell^+\ell^-)$ with $q^2 \in [1, 6]$ GeV.
[Buchalla, Isidori, Rey, NPB 511 (1998) 594]

More on resolved photons in $\bar{B} \to X_s\gamma$ and $\bar{B} \to X_s\ell^+\ell^-$

Background-subtracted $\bar{B} \to X_{s+d}\,\gamma$ photon energy spectrum in the $\Upsilon(4S)$ rest frame, from Fig. 1 of the Belle analysis in arXiv:1608.02344.

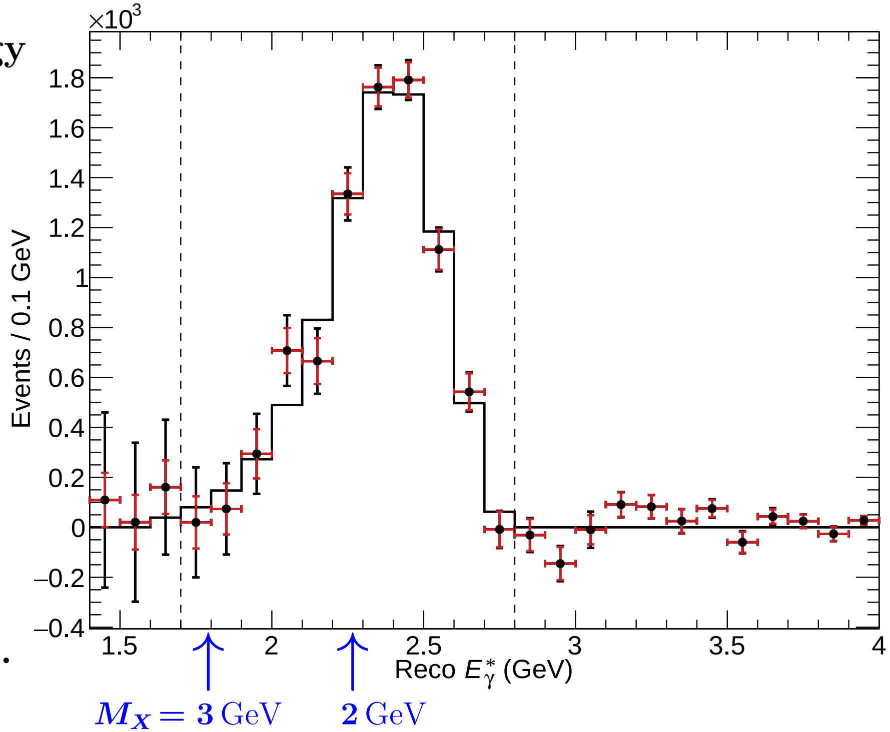

For $M_X \lesssim 3\,\text{GeV}$ and in the absence of 4-quark ops, we have local OPE $\Rightarrow \mathcal{O}(\Lambda^2/m_b^2)$.

In the presence of 4-quark ops:
Light quark loops – suppressed by $C_{3,\ldots,6}$ or CKM;
Charm loops – factorizable or local if m_c^2 is sufficiently large w.r.t. $m_b\Lambda$. Numerically, $\mathcal{O}(3\%)$ non-fact. effects found in $\mathcal{B}(\bar{B} \to X_s\gamma)$ and $\mathcal{B}(\bar{B} \to X_s\ell^+\ell^-)$ with $q^2 \in [1, 6]\,\text{GeV}$.
[Buchalla, Isidori, Rey, NPB 511 (1998) 594]

However, m_c^2 is not sufficiently large $\Rightarrow$ Treat it as $\mathcal{O}(m_b\Lambda)$ and use SCET, so far up to $\mathcal{O}(\Lambda/m_b)$:
For $\mathcal{B}(\bar{B} \to X_s\gamma)$ with $E_\gamma > 1.6\,\text{GeV}$ [Benzke, Lee, Neubert, Paz, JHEP 1008 (2010) 099] $[-4.8\%, +5.6\%]$ uncert. range.
For $\mathcal{B}(\bar{B} \to X_s\ell^+\ell^-)$ with $q^2 \in [1, 6]\,\text{GeV}$ [Benzke, Hurth, Turczyk, JHEP 1710 (2017) 031] $[-2.7\%, +1.8\%]$ range.
(On the top of the factorizable and/or local effects, including the Λ^2/m_c^2 ones.)

More on resolved photons in $\bar{B} \to X_s\gamma$ and $\bar{B} \to X_s\ell^+\ell^-$

Background-subtracted $\bar{B} \to X_{s+d}\gamma$ photon energy spectrum in the $\Upsilon(4S)$ rest frame, from Fig. 1 of the Belle analysis in arXiv:1608.02344.

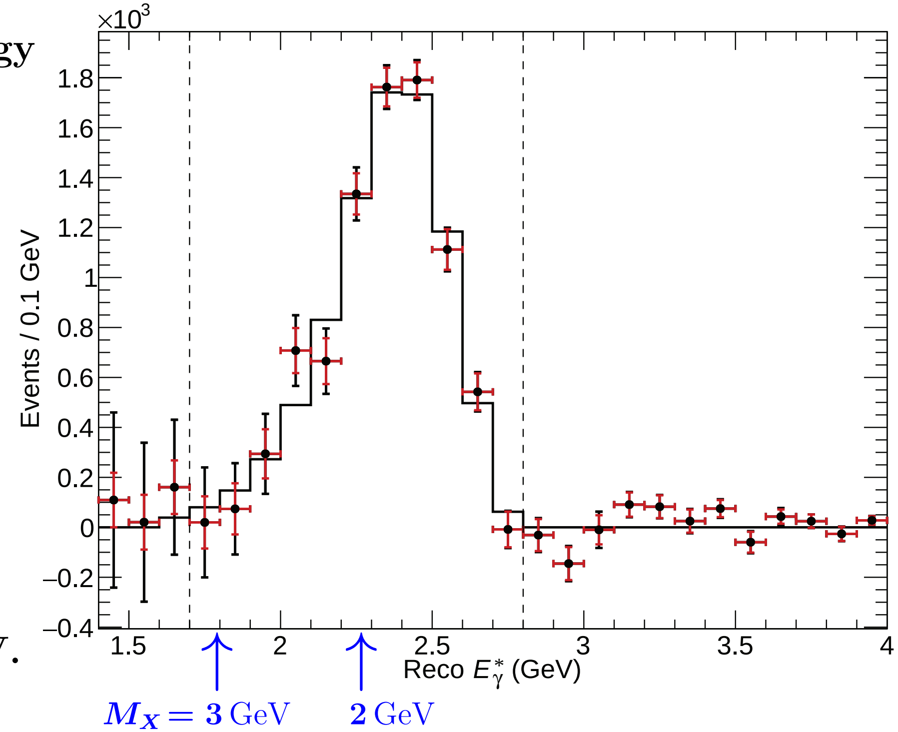

For $M_X \lesssim 3\,\text{GeV}$ and in the absence of 4-quark ops, we have local OPE $\Rightarrow \mathcal{O}(\Lambda^2/m_b^2)$.

In the presence of 4-quark ops:
Light quark loops – suppressed by $C_{3,\ldots,6}$ or CKM;
Charm loops – factorizable or local if m_c^2 is sufficiently large w.r.t. $m_b\Lambda$. Numerically, $\mathcal{O}(3\%)$ non-fact. effects found in $\mathcal{B}(\bar{B} \to X_s\gamma)$ and $\mathcal{B}(\bar{B} \to X_s\ell^+\ell^-)$ with $q^2 \in [1,6]\,\text{GeV}$.
[Buchalla, Isidori, Rey, NPB 511 (1998) 594]

However, m_c^2 is not sufficiently large $\Rightarrow$ Treat it as $\mathcal{O}(m_b\Lambda)$ and use SCET, so far up to $\mathcal{O}(\Lambda/m_b)$:
For $\mathcal{B}(\bar{B} \to X_s\gamma)$ with $E_\gamma > 1.6\,\text{GeV}$ [Benzke, Lee, Neubert, Paz, JHEP 1008 (2010) 099] $[-4.8\%, +5.6\%]$ uncert. range.
For $\mathcal{B}(\bar{B} \to X_s\ell^+\ell^-)$ with $q^2 \in [1,6]\,\text{GeV}$ [Benzke, Hurth, Turczyk, JHEP 1710 (2017) 031] $[-2.7\%, +1.8\%]$ range.
(On the top of the factorizable and/or local effects, including the Λ^2/m_c^2 ones.)

Corrections not involving Q_7 and Q_8 are of higher order, i.e. $\mathcal{O}\left[\left(\frac{\Lambda}{m_b}\right)^a\right]$ with $a \geq \frac{3}{2}$ and/or $\mathcal{O}\left(\frac{\alpha_s\Lambda}{m_b}\right)$.
That's what we miss using the purely perturbative expression for $\left|C_9^{\text{eff}}(q^2)\right|^2$ and the local $1/m_c^2$ effects.
However, the applied SCET power counting works only for small M_X and small q^2 – verte.

SCET power counting in the $\bar{B} \to X_s \ell^+ \ell^-$ analysis of Benzke, Hurth and Turczyk, JHEP 1710 (2017) 031.

$\lambda = \frac{\Lambda}{M_B}$, $\quad M_X \lesssim \sqrt{M_B \Lambda} = M_B \sqrt{\lambda} \sim m_c.$

$$a^\mu = \frac{1}{2}(na)\bar{n}^\mu + \frac{1}{2}(\bar{n}a)n^\mu + a_\perp^\mu, \quad \text{with} \quad n^\mu = \begin{bmatrix} 1 \\ 0 \\ 0 \\ 1 \end{bmatrix}^\mu, \quad \bar{n}^\mu = \begin{bmatrix} 1 \\ 0 \\ 0 \\ -1 \end{bmatrix}^\mu.$$

$\uparrow$
any vector

In the plot $\quad q_\perp = 0 \quad \Rightarrow \quad q^2 = (\bar{n}q)(nq).$

hard:	$p \sim (1, 1, 1)\, M_B,$
hard-collinear:	$p \sim (\lambda, 1, \sqrt{\lambda})\, M_B,$
anti-hard-collinear:	$p \sim (1, \lambda, \sqrt{\lambda})\, M_B,$
soft:	$p \sim (\lambda, \lambda, \lambda)\, M_B.$

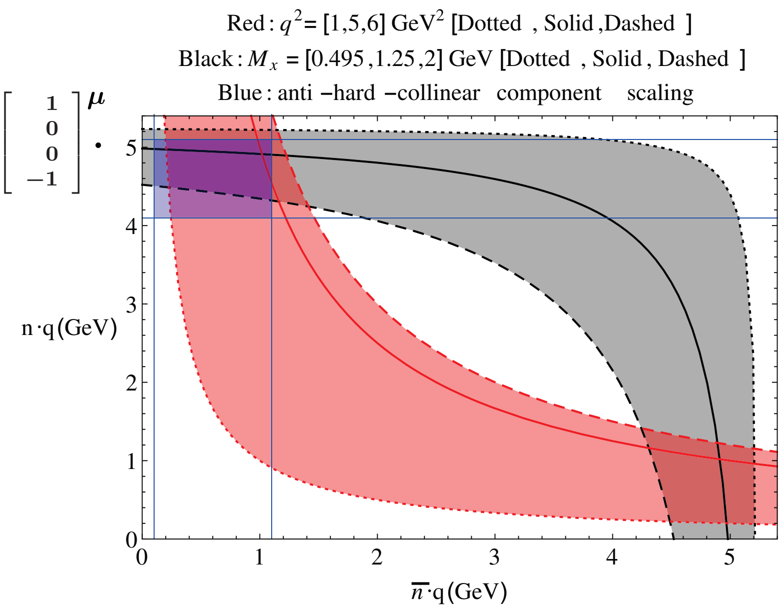

SCET power counting in the $\bar{B} \to X_s \ell^+ \ell^-$ analysis of Benzke, Hurth and Turczyk, JHEP 1710 (2017) 031.

$\lambda = \frac{\Lambda}{M_B}, \quad M_X \lesssim \sqrt{M_B \Lambda} = M_B \sqrt{\lambda} \sim m_c.$

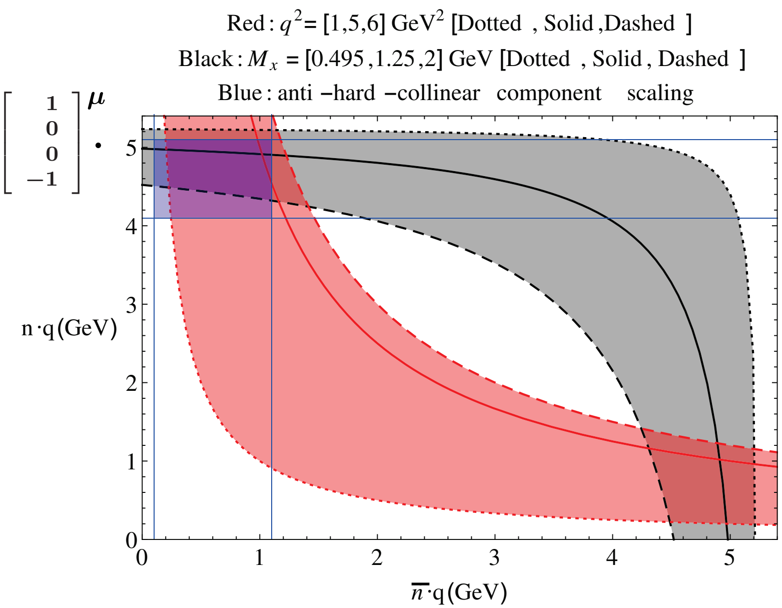

$a^\mu = \frac{1}{2}(na)\bar{n}^\mu + \frac{1}{2}(\bar{n}a)n^\mu + a_\perp^\mu,$ with $n^\mu = \begin{bmatrix} 1 \\ 0 \\ 0 \\ 1 \end{bmatrix}^\mu, \quad \bar{n}^\mu = \begin{bmatrix} 1 \\ 0 \\ 0 \\ -1 \end{bmatrix}^\mu.$

$\uparrow$

any vector

In the plot $q_\perp = 0 \quad \Rightarrow \quad q^2 = (\bar{n}q)(nq).$

hard:	$p \sim (1, 1, 1)\, M_B,$
hard-collinear:	$p \sim (\lambda, 1, \sqrt{\lambda})\, M_B,$
anti-hard-collinear:	$p \sim (1, \lambda, \sqrt{\lambda})\, M_B,$
soft:	$p \sim (\lambda, \lambda, \lambda)\, M_B.$

Plot $\Rightarrow$ Our cuts would better fit into the SCET-accessible region if we restricted to $q^2 \in [1, 5]$ GeV. On the other hand, the cut on M_X could be somewhat larger than 2 GeV.

SCET power counting in the $\bar{B} \to X_s \ell^+ \ell^-$ analysis of Benzke, Hurth and Turczyk, JHEP 1710 (2017) 031.

$\lambda = \frac{\Lambda}{M_B}$, $\quad M_X \lesssim \sqrt{M_B \Lambda} = M_B \sqrt{\lambda} \sim m_c.$

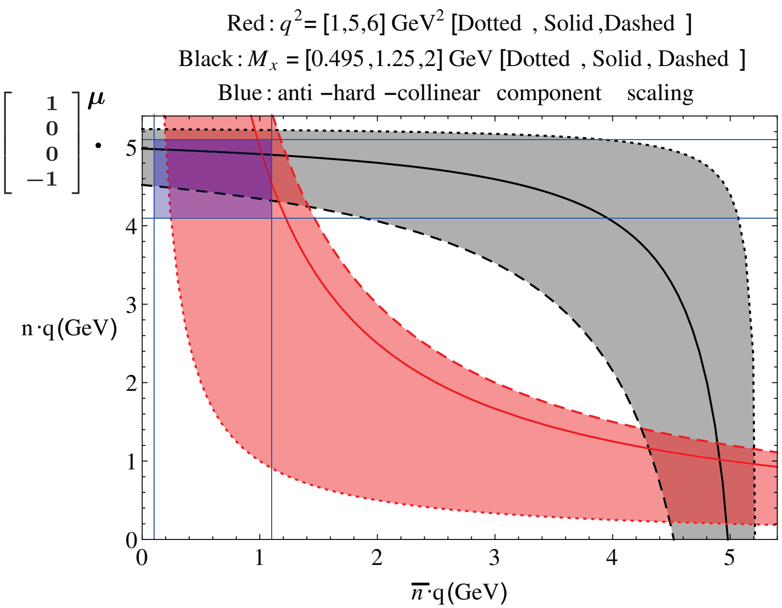

$$a^\mu = \frac{1}{2}(na)\bar{n}^\mu + \frac{1}{2}(\bar{n}a)n^\mu + a_\perp^\mu, \quad \text{with} \quad n^\mu = \begin{bmatrix} 1 \\ 0 \\ 0 \\ 1 \end{bmatrix}^\mu, \quad \bar{n}^\mu = \begin{bmatrix} 1 \\ 0 \\ 0 \\ -1 \end{bmatrix}^\mu.$$

$\uparrow$ any vector

In the plot $\quad q_\perp = 0 \quad \Rightarrow \quad q^2 = (\bar{n}q)(nq).$

hard:	$p \sim (1, 1, 1)\, M_B,$
hard-collinear:	$p \sim (\lambda, 1, \sqrt{\lambda})\, M_B,$
anti-hard-collinear:	$p \sim (1, \lambda, \sqrt{\lambda})\, M_B,$
soft:	$p \sim (\lambda, \lambda, \lambda)\, M_B.$

Plot $\Rightarrow$ Our cuts would better fit into the SCET-accessible region if we restricted to $q^2 \in [1, 5]$ GeV. On the other hand, the cut on M_X could be somewhat larger than 2 GeV.

The factorization formula:

$$d\Gamma = \sum_{n=0}^{\infty} \frac{1}{m_b^n} \sum_i H_i^{(n)} J_i^{(n)} \otimes S_i^{(n)} + \sum_{n=1}^{\infty} \frac{1}{m_b^n} \left[\sum_i H_i^{(n)} J_i^{(n)} \otimes S_i^{(n)} \otimes \bar{J}_i^{(n)} + \sum_i H_i^{(n)} J_i^{(n)} \otimes S_i^{(n)} \otimes \bar{J}_i^{(n)} \otimes \bar{J}_i^{(n)} \right]$$

SCET power counting in the $\bar{B} \to X_s \ell^+ \ell^-$ analysis of Benzke, Hurth and Turczyk, JHEP 1710 (2017) 031.

$\lambda = \frac{\Lambda}{M_B}, \quad M_X \lesssim \sqrt{M_B \Lambda} = M_B \sqrt{\lambda} \sim m_c.$

$a^\mu = \frac{1}{2}(na)\bar{n}^\mu + \frac{1}{2}(\bar{n}a)n^\mu + a_\perp^\mu$, with $n^\mu = \begin{bmatrix} 1 \\ 0 \\ 0 \\ 1 \end{bmatrix}^\mu, \quad \bar{n}^\mu = \begin{bmatrix} 1 \\ 0 \\ 0 \\ -1 \end{bmatrix}^\mu.$

$\uparrow$
any vector

In the plot $q_\perp = 0 \quad \Rightarrow \quad q^2 = (\bar{n}q)(nq).$

hard:	$p \sim (1, 1, 1)\, M_B,$
hard-collinear:	$p \sim (\lambda, 1, \sqrt{\lambda})\, M_B,$
anti-hard-collinear:	$p \sim (1, \lambda, \sqrt{\lambda})\, M_B,$
soft:	$p \sim (\lambda, \lambda, \lambda)\, M_B.$

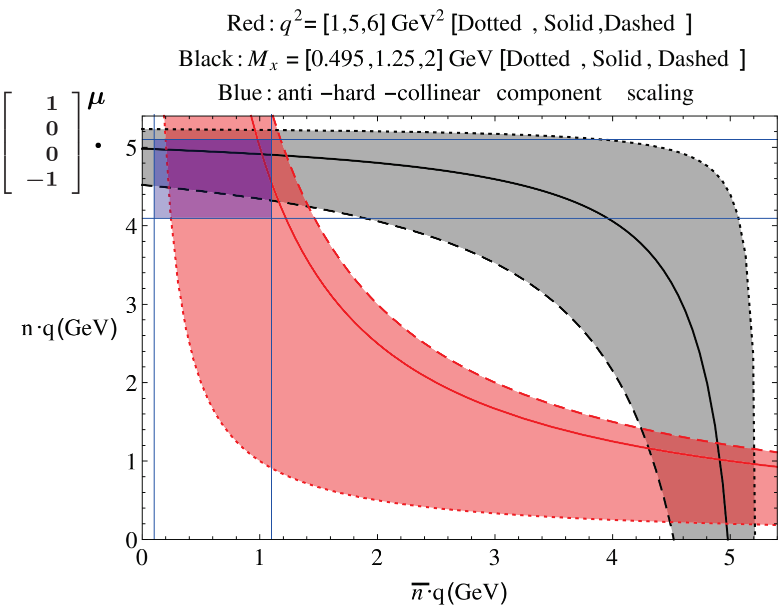

Plot $\Rightarrow$ Our cuts would better fit into the SCET-accessible region if we restricted to $q^2 \in [1, 5]\,$GeV. On the other hand, the cut on M_X could be somewhat larger than $2\,$GeV.

The factorization formula:

$$d\Gamma = \sum_{n=0}^{\infty} \frac{1}{m_b^n} \sum_i H_i^{(n)} J_i^{(n)} \otimes S_i^{(n)} + \sum_{n=1}^{\infty} \frac{1}{m_b^n} \left[\sum_i H_i^{(n)} J_i^{(n)} \otimes S_i^{(n)} \otimes \bar{J}_i^{(n)} + \sum_i H_i^{(n)} J_i^{(n)} \otimes S_i^{(n)} \otimes \bar{J}_i^{(n)} \otimes \bar{J}_i^{(n)} \right]$$

Remarks:

1. Not proven. Contradictions observed in the $Q_8 - Q_8$ case, claimed to be phenomenologically irrelevant.
2. Relates unknowns to unknowns. Models of soft functions needed (constraints available).
3. Corrections beyond $\mathcal{O}(\Lambda/M_B)$ are likely to be relevant because $|C_{9,10}/C_7| \sim 13$ (work in progress) [BHT].
4. Other observables – after including the above corrections.
5. Different power counting than in the previous SCET analyses where no "resolved photons" were included [Lee, Stewart, PRD74 (2006) 014005], [Bell, Beneke, Huber, Li, NPB843 (2011) 143].

The $b \to s\gamma$ spectrum

Gambino, Lunghi, Misiak, Schacht
in progress

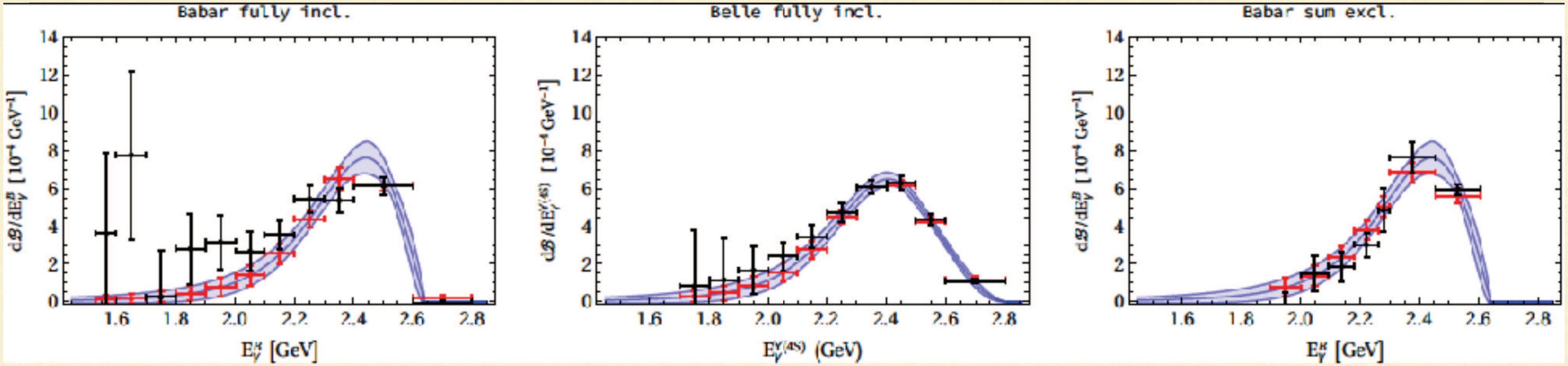

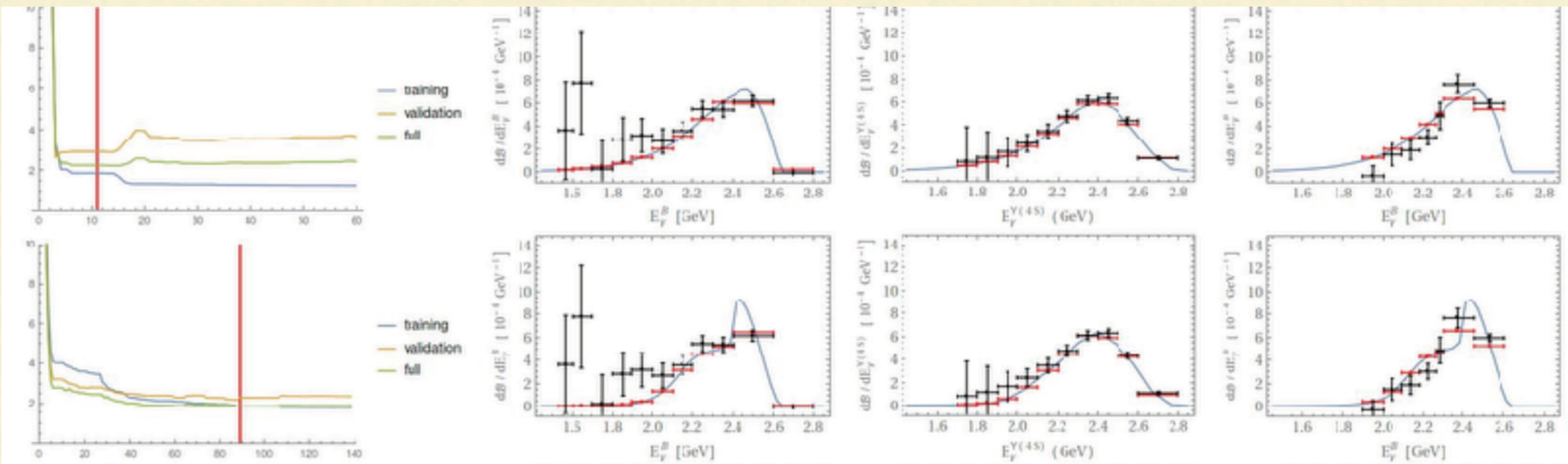

Up-to-date theoretical description of spectrum to get leading SF and reliable extrapolation to low cuts.

NNLO QCD corrections to $\bar{B} \to X_s \gamma$

The relevant perturbative quantity $P(E_0)$:

$$\frac{\Gamma[b \to X_s \gamma]_{E_\gamma > E_0}}{\Gamma[b \to X_u e \bar{\nu}]} = \left| \frac{V_{ts}^* V_{tb}}{V_{ub}} \right|^2 \frac{6 \alpha_{\rm em}}{\pi} \underbrace{\sum_{i,j} C_i(\mu_b)\, C_j(\mu_b)\, K_{ij}}_{P(E_0)}$$

NNLO QCD corrections to $\bar{B} \to X_s \gamma$

The relevant perturbative quantity $P(E_0)$:

$$\frac{\Gamma[b \to X_s \gamma]_{E_\gamma > E_0}}{\Gamma[b \to X_u e \bar{\nu}]} = \left| \frac{V_{ts}^* V_{tb}}{V_{ub}} \right|^2 \frac{6\alpha_{\rm em}}{\pi} \underbrace{\sum_{i,j} C_i(\mu_b)\, C_j(\mu_b)\, K_{ij}}_{P(E_0)}$$

Expansions of the Wilson coefficients and K_{ij} in $\widetilde{\alpha}_s \equiv \frac{\alpha_s(\mu_b)}{4\pi}$:

$$C_i(\mu_b) = C_i^{(0)} + \widetilde{\alpha}_s\, C_i^{(1)} + \widetilde{\alpha}_s^2\, C_i^{(2)} + \ldots$$

$$K_{ij} = K_{ij}^{(0)} + \widetilde{\alpha}_s\, K_{ij}^{(1)} + \widetilde{\alpha}_s^2\, K_{ij}^{(2)} + \ldots$$

NNLO QCD corrections to $\bar{B} \to X_s \gamma$

The relevant perturbative quantity $P(E_0)$:

$$\frac{\Gamma[b \to X_s \gamma]_{E_\gamma > E_0}}{\Gamma[b \to X_u e \bar{\nu}]} = \left| \frac{V_{ts}^* V_{tb}}{V_{ub}} \right|^2 \frac{6\alpha_{\rm em}}{\pi} \underbrace{\sum_{i,j} C_i(\mu_b)\, C_j(\mu_b)\, K_{ij}}_{P(E_0)}$$

Expansions of the Wilson coefficients and K_{ij} in $\widetilde{\alpha}_s \equiv \frac{\alpha_s(\mu_b)}{4\pi}$:

$$C_i(\mu_b) = C_i^{(0)} + \widetilde{\alpha}_s\, C_i^{(1)} + \widetilde{\alpha}_s^2\, C_i^{(2)} + \ldots$$

$$K_{ij} = K_{ij}^{(0)} + \widetilde{\alpha}_s\, K_{ij}^{(1)} + \widetilde{\alpha}_s^2\, K_{ij}^{(2)} + \ldots$$

Most important at the NNLO: $K_{77}^{(2)}$, $K_{27}^{(2)}$ and $K_{17}^{(2)}$.

They depend on $\frac{\mu_b}{m_b}$, $\delta = 1 - \frac{2E_0}{m_b}$ and $z = \frac{m_c^2}{m_b^2}$.

Towards complete $K_{17}^{(2)}$ and $K_{27}^{(2)}$ for arbitrary m_c

[MM, A. Rehman, M. Steinhauser, ...]
in progress

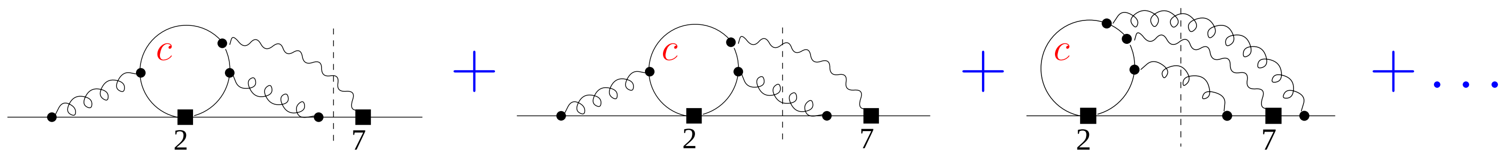

Towards complete $K_{17}^{(2)}$ and $K_{27}^{(2)}$ for arbitrary m_c

[MM, A. Rehman, M. Steinhauser, ...]
in progress

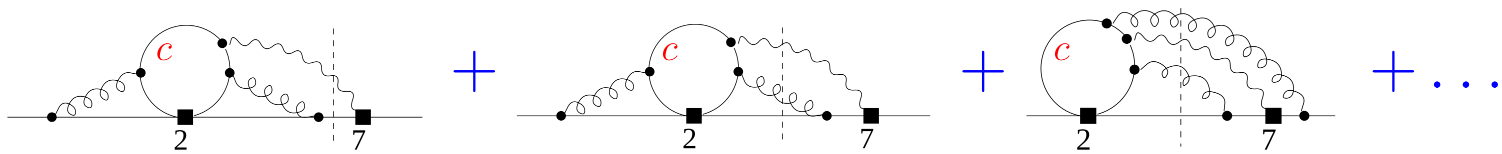

1. **Generation of diagrams and performing the Dirac algebra to express everything in terms of 585309 four-loop two-scale scalar integrals with unitarity cuts (437 families).**

Towards complete $K_{17}^{(2)}$ and $K_{27}^{(2)}$ for arbitrary m_c

[MM, A. Rehman, M. Steinhauser, ...]
in progress

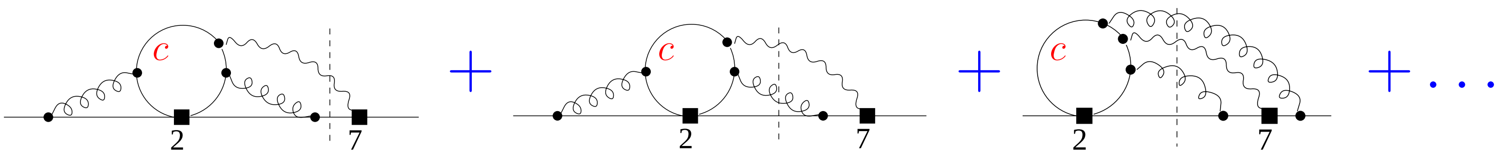

$+$ $+$ $+ \ldots$

1. **Generation of diagrams and performing the Dirac algebra to express everything in terms of 585309 four-loop two-scale scalar integrals with unitarity cuts (437 families).**

2. **Reduction to master integrals with the help of Integration By Parts (IBP).**

   Available public C++ codes: **REDUZE** **[C. Studerus, arXiv:0912.2546],**
   FIRE **[A.V. Smirnov, arXiv:1408.2372].**

   A useful Mathematica code: **LiteRed** **[R.N. Lee, arXiv:1212.2685]** **(symmetries...).**

   At the moment (MM), 147 families (166509 integrals) still await for reduction.

   Expected needs for the most difficult families: 1 TB RAM & 1 month CPU.

Towards complete $K_{17}^{(2)}$ and $K_{27}^{(2)}$ for arbitrary m_c [MM, A. Rehman, M. Steinhauser, ...] in progress

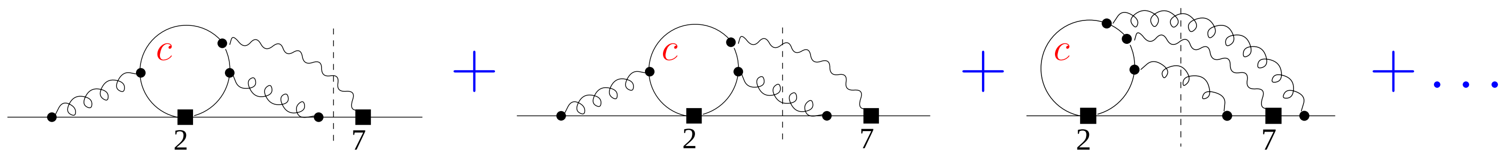

1. Generation of diagrams and performing the Dirac algebra to express everything in terms of 585309 four-loop two-scale scalar integrals with unitarity cuts (437 families).

2. Reduction to master integrals with the help of Integration By Parts (IBP).

   Available public C++ codes: REDUZE [C. Studerus, arXiv:0912.2546], FIRE [A.V. Smirnov, arXiv:1408.2372].

   A useful Mathematica code: LiteRed [R.N. Lee, arXiv:1212.2685] (symmetries...).

   At the moment (MM), 147 families (166509 integrals) still await for reduction.

   Expected needs for the most difficult families: 1 TB RAM & 1 month CPU.

3. Extending the set of master integrals I_n so that it closes under differentiation with respect to $z = m_c^2/m_b^2$. This way one obtains a system of differential equations

$$\frac{d}{dz} I_n = \Sigma_k \, w_{nk}(z, \epsilon) \, I_k, \qquad (*)$$

   where w_{nk} are rational functions of their arguments.

Towards complete $K_{17}^{(2)}$ and $K_{27}^{(2)}$ for arbitrary m_c

[MM, A. Rehman, M. Steinhauser, …]
in progress

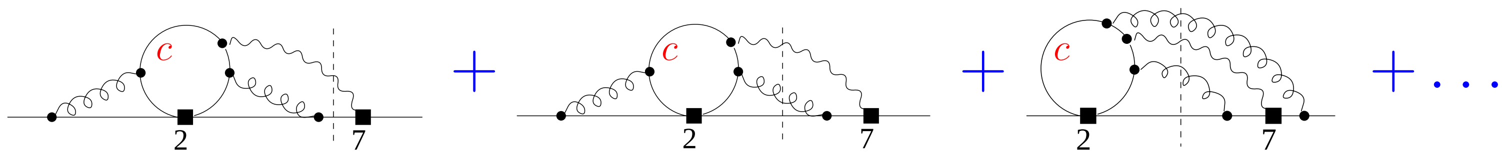

1. Generation of diagrams and performing the Dirac algebra to express everything in terms of 585309 four-loop two-scale scalar integrals with unitarity cuts (437 families).

2. Reduction to master integrals with the help of Integration By Parts (IBP).

   Available public C++ codes: REDUZE [C. Studerus, arXiv:0912.2546], FIRE [A.V. Smirnov, arXiv:1408.2372].

   A useful Mathematica code: LiteRed [R.N. Lee, arXiv:1212.2685] (symmetries...).

   At the moment (MM), 147 families (166509 integrals) still await for reduction.

   Expected needs for the most difficult families: 1 TB RAM & 1 month CPU.

3. Extending the set of master integrals I_n so that it closes under differentiation with respect to $z = m_c^2/m_b^2$. This way one obtains a system of differential equations

$$\frac{d}{dz} I_n = \Sigma_k \, w_{nk}(z, \epsilon) \, I_k, \qquad (*)$$

   where w_{nk} are rational functions of their arguments.

4. Calculating boundary conditions for $(*)$ using automatized asymptotic expansions at $m_c \gg m_b$.

Towards complete $K_{17}^{(2)}$ and $K_{27}^{(2)}$ for arbitrary m_c

[MM, A. Rehman, M. Steinhauser, ...]
in progress

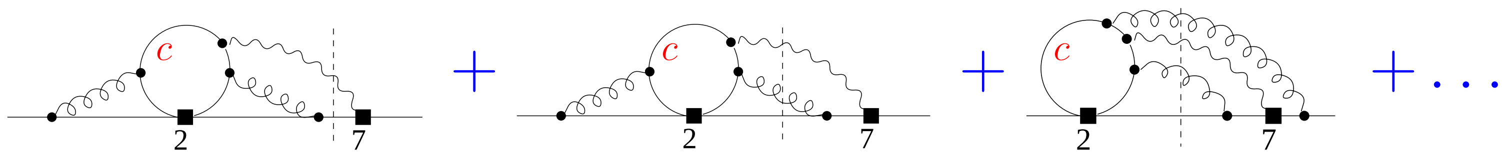

1. Generation of diagrams and performing the Dirac algebra to express everything in terms of 585309 four-loop two-scale scalar integrals with unitarity cuts (437 families).

2. Reduction to master integrals with the help of Integration By Parts (IBP).

   Available public C++ codes: REDUZE [C. Studerus, arXiv:0912.2546],
   FIRE [A.V. Smirnov, arXiv:1408.2372].
   A useful Mathematica code: LiteRed [R.N. Lee, arXiv:1212.2685] (symmetries...).

   At the moment (MM), 147 families (166509 integrals) still await for reduction.

   Expected needs for the most difficult families: 1 TB RAM & 1 month CPU.

3. Extending the set of master integrals I_n so that it closes under differentiation with respect to $z = m_c^2/m_b^2$. This way one obtains a system of differential equations

$$\frac{d}{dz} I_n = \Sigma_k \, w_{nk}(z,\epsilon) \, I_k, \qquad (*)$$

   where w_{nk} are rational functions of their arguments.

4. Calculating boundary conditions for $(*)$ using automatized asymptotic expansions at $m_c \gg m_b$.

5. Calculating three-loop single-scale master integrals for the boundary conditions. Methods ...

Towards complete $K_{17}^{(2)}$ and $K_{27}^{(2)}$ for arbitrary m_c

[MM, A. Rehman, M. Steinhauser, ...]
in progress

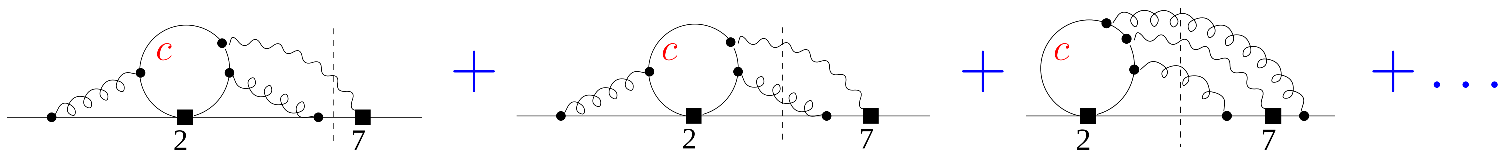

1. Generation of diagrams and performing the Dirac algebra to express everything in terms of 585309 four-loop two-scale scalar integrals with unitarity cuts (437 families).

2. Reduction to master integrals with the help of Integration By Parts (IBP).

   Available public C++ codes: REDUZE [C. Studerus, arXiv:0912.2546],
   FIRE [A.V. Smirnov, arXiv:1408.2372].

   A useful Mathematica code: LiteRed [R.N. Lee, arXiv:1212.2685] (symmetries...).

   At the moment (MM), 147 families (166509 integrals) still await for reduction.

   Expected needs for the most difficult families: 1 TB RAM & 1 month CPU.

3. Extending the set of master integrals I_n so that it closes under differentiation with respect to $z = m_c^2/m_b^2$. This way one obtains a system of differential equations

$$\frac{d}{dz} I_n = \Sigma_k \, w_{nk}(z,\epsilon) \, I_k, \qquad (*)$$

   where w_{nk} are rational functions of their arguments.

4. Calculating boundary conditions for $(*)$ using automatized asymptotic expansions at $m_c \gg m_b$.

5. Calculating three-loop single-scale master integrals for the boundary conditions. Methods ...

6. Solving the system $(*)$ numerically [A.C. Hindmarsch, `http://www.netlib.org/odepack`] along an ellipse in the complex z plane. Doing so along several different ellipses allows us to estimate the numerical error.

Summary

- The Belle measurement of isospin asymmetry in $\bar{B} \to X_s\gamma$ helps to suppress non-perturbative uncertainties in the theoretical prediction for the branching ratio.

Summary

- The Belle measurement of isospin asymmetry in $\bar{B} \to X_s \gamma$ helps to suppress non-perturbative uncertainties in the theoretical prediction for the branching ratio.

- Charm quark loops in the inclusive $\bar{B} \to X_s \ell^+ \ell^-$ decay seem to be under better control than in the corresponding exclusive decays.
  $\Rightarrow$ Handle on C_9 even if the absence of LFU violation.

Summary

- The Belle measurement of isospin asymmetry in $\bar{B} \to X_s\gamma$ helps to suppress non-perturbative uncertainties in the theoretical prediction for the branching ratio.

- Charm quark loops in the inclusive $\bar{B} \to X_s\ell^+\ell^-$ decay seem to be under better control than in the corresponding exclusive decays.
  $\Rightarrow$ Handle on C_9 even if the absence of LFU violation.

- Extrapolation in M_{X_s} and/or E_γ requires further work on fitting generic shape-function models to currently available experimental data.

Summary

- The Belle measurement of isospin asymmetry in $\bar{B} \to X_s\gamma$ helps to suppress non-perturbative uncertainties in the theoretical prediction for the branching ratio.

- Charm quark loops in the inclusive $\bar{B} \to X_s\ell^+\ell^-$ decay seem to be under better control than in the corresponding exclusive decays.
$\Rightarrow$ Handle on C_9 even if the absence of LFU violation.

- Extrapolation in M_{X_s} and/or E_γ requires further work on fitting generic shape-function models to currently available experimental data.

- Perturbative calculations of $\bar{B} \to X_s\gamma$ require further optimization of software/hardware for the IBP reduction.

BACKUP SLIDES

Information on electroweak-scale physics in the $b \to s\gamma$ transition is encoded in an effective low-energy local interaction:

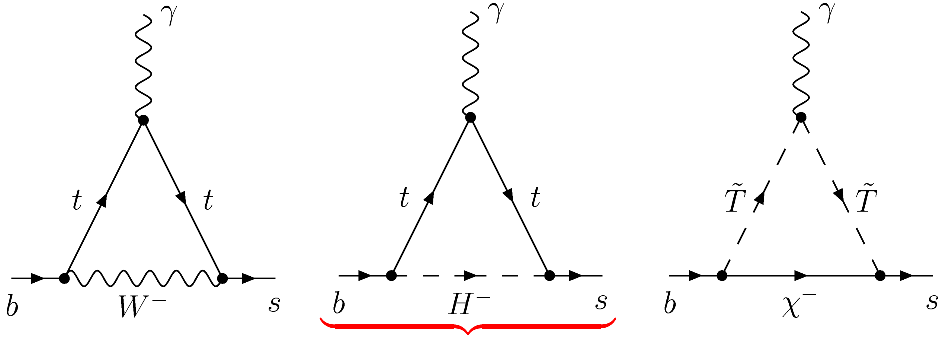

$\Rightarrow M_{H^\pm} > \sim 500\,\mathbf{GeV}$

in the 2HDM-II

$\longrightarrow$

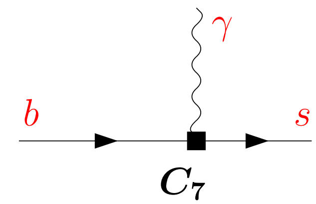

$$b \in \bar{B} \equiv (\bar{B}^0 \text{ or } B^-)$$

Information on electroweak-scale physics in the $b \to s\gamma$ transition is encoded in an effective low-energy local interaction:

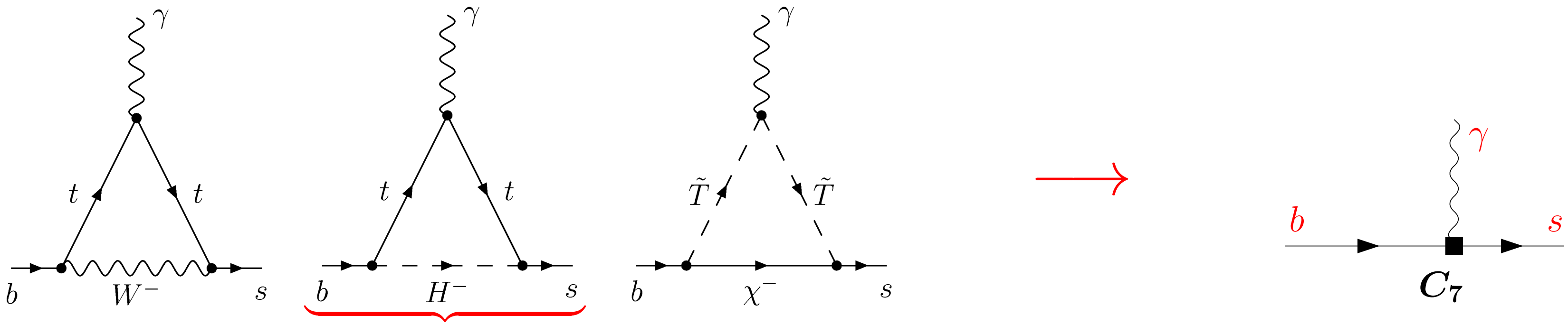

$\Rightarrow M_{H^\pm} > \sim 500\,\text{GeV}$
in the 2HDM-II

$b \in \bar{B} \equiv (\bar{B}^0 \text{ or } B^-)$

The inclusive $\bar{B} \to X_s\gamma$ decay rate for $E_\gamma > E_0$ is well approximated by the corresponding perturbative decay rate of the b-quark:

$$\Gamma(\bar{B} \to X_s\gamma) \;=\; \Gamma(b \to X_s^p\gamma) \;+ \left(\begin{array}{c}\text{non-perturbative effects}\\ (3\pm 5)\%\end{array}\right)$$

[G. Buchalla, G. Isidori and S.-J. Rey, Nucl. Phys. B511 (1998) 594]
[M. Benzke, S.J. Lee, M. Neubert and G. Paz, JHEP 1008 (2010) 099]
(BLNP)

provided E_0 is large $(E_0 \sim m_b/2)$
but not too close to the endpoint $(m_b - 2E_0 \gg \Lambda_{\rm QCD})$.

Conventionally, $E_0 = 1.6\,\text{GeV} \simeq m_b/3$ is chosen.

Decoupling of W, Z, t, H^0 $\Rightarrow$ effective weak interaction Lagrangian:

$$L_{\mathrm{weak}} \sim \sum_i C_i Q_i$$

Eight operators Q_i matter for $\mathcal{B}_{s\gamma}^{\mathrm{SM}}$ when the NLO EW and/or CKM-suppressed effects are neglected:

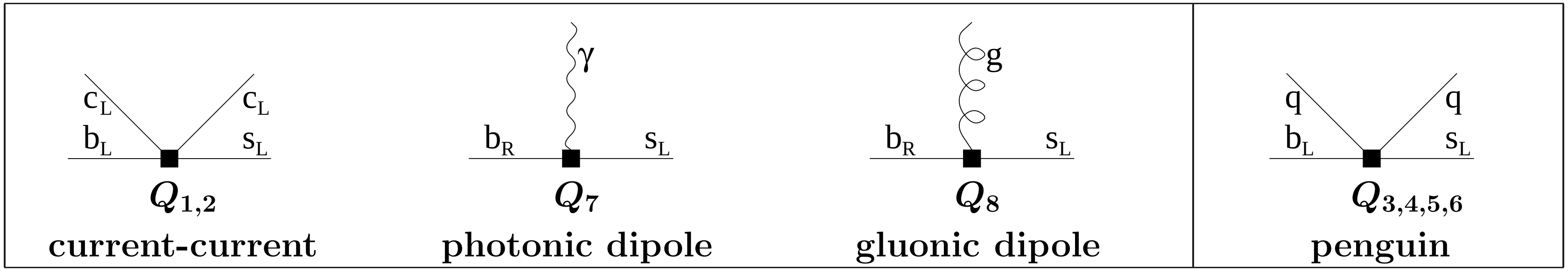

Decoupling of W, Z, t, H^0 $\Rightarrow$ effective weak interaction Lagrangian:

$$L_{\mathrm{weak}} \sim \sum_i C_i Q_i$$

Eight operators Q_i matter for $\mathcal{B}_{s\gamma}^{\mathrm{SM}}$ when the NLO EW and/or CKM-suppressed effects are neglected:

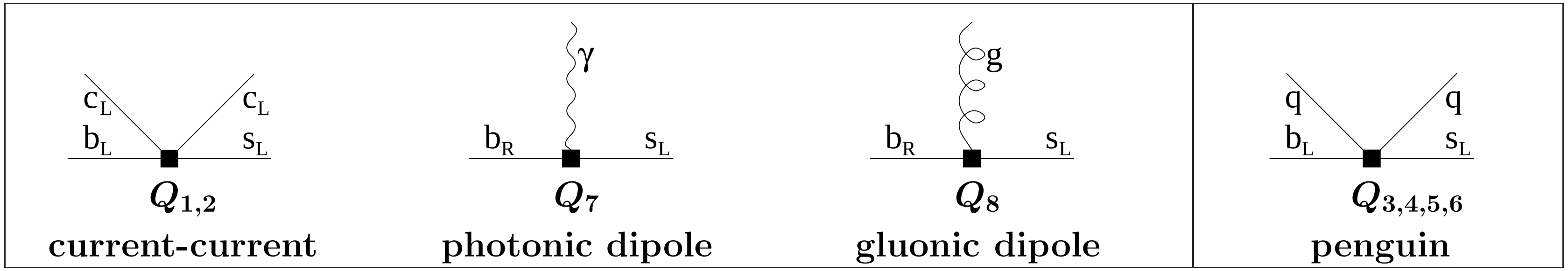

$$\Gamma(\bar{B} \to X_s\gamma)_{E_\gamma > E_0} = |C_7(\mu_b)|^2\, \Gamma_{77}(E_0) + (\text{other}) \qquad (\mu_b \sim m_b/2)$$

Optical theorem:

$$\frac{d\Gamma_{77}}{dE_\gamma} \sim \mathrm{Im}\{\ \cdots\ \} \equiv \mathrm{Im}\, A$$

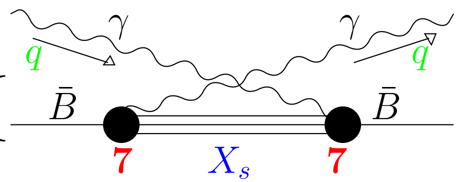

Integrating the amplitude A over E_γ:

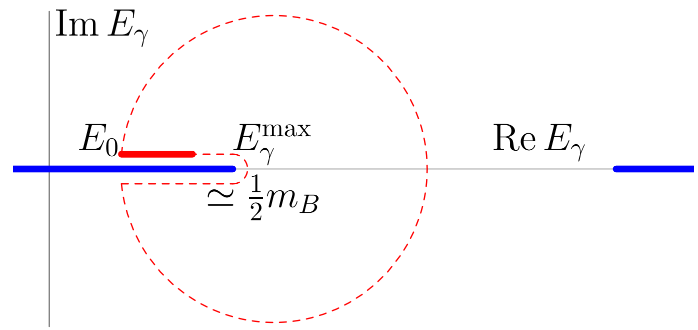

OPE on the ring $\Rightarrow$ **Non-perturbative corrections to $\Gamma_{77}(E_0)$ form a series in $\frac{\Lambda_{\mathrm{QCD}}}{m_b}$ and α_s that begins with**

$$\frac{\mu_\pi^2}{m_b^2},\ \frac{\mu_G^2}{m_b^2},\ \frac{\rho_D^3}{m_b^3},\ \frac{\rho_{LS}^3}{m_b^3}, \ldots;\ \frac{\alpha_s \mu_\pi^2}{(m_b - 2E_0)^2},\ \frac{\alpha_s \mu_G^2}{m_b(m_b - 2E_0)}; \ldots,$$

where $\mu_\pi, \mu_G, \rho_D, \rho_{LS} = \mathcal{O}(\Lambda_{\mathrm{QCD}})$ are extracted from the semileptonic $\bar{B} \to X_c e \bar{\nu}$ spectra and the B–$B^\star$ mass difference.

The same method has been applied to the 3-loop counterterm diagrams

[MM, A. Rehman, M. Steinhauser, PLB 770 (2017) 431]

Master integrals:

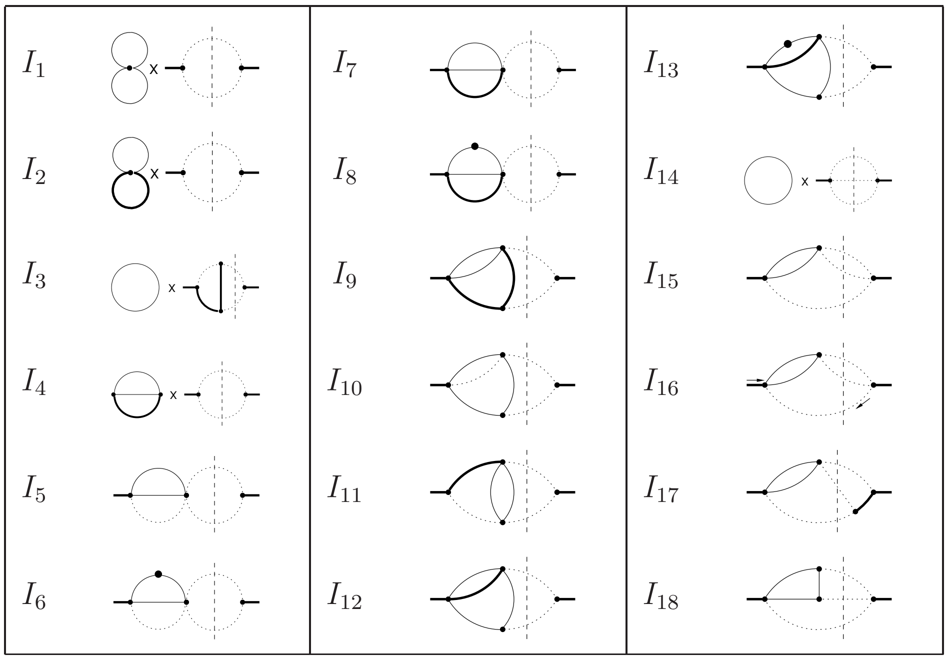

Results for the bare NLO contributions up to $\mathcal{O}(\epsilon)$:

$$\hat{G}_{27}^{(1)2P} = -\frac{92}{81\epsilon} + f_0(z) + \epsilon f_1(z) \xrightarrow{z\to 0} -\frac{92}{81\epsilon} - \frac{1942}{243} + \epsilon\left(-\frac{26231}{729} + \frac{259}{243}\pi^2\right)$$

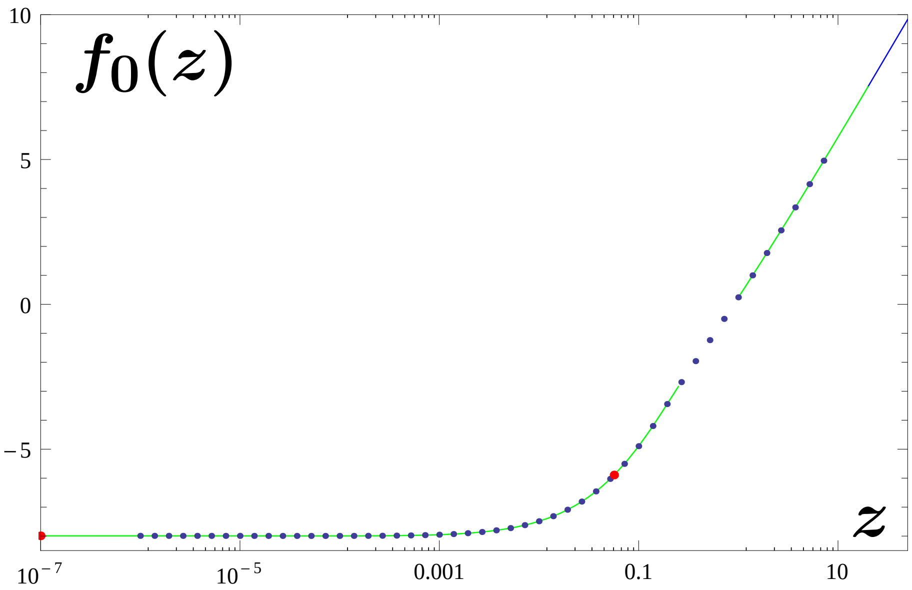

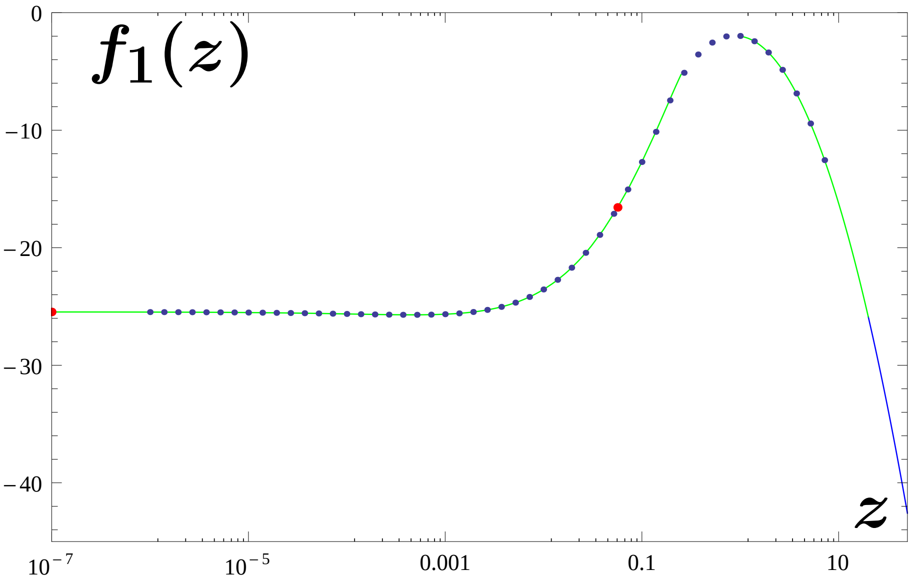

Dots: solutions to the differential equations and/or the exact $z \to 0$ limit.
Lines: large- and small-z asymptotic expansions

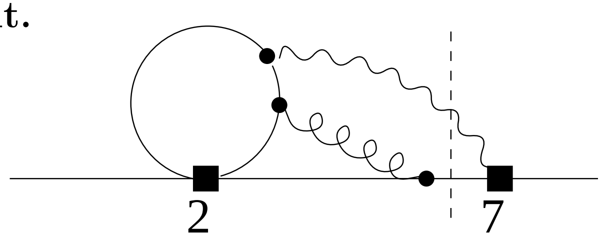

Small-z expansions of $\hat{G}_{27}^{(1)2P}$:

f_0 from **C. Greub, T. Hurth, D. Wyler, hep-ph/9602281, hep-ph/9603404,**
A. J. Buras, A. Czarnecki, MM, J. Urban, hep-ph/0105160,

f_1 from **H.M. Asatrian, C. Greub, A. Hovhannisyan, T. Hurth and V. Poghosyan, hep-ph/0505068.**

Analogous results for the 3-body final state contributions ($\delta = 1$):

$$\hat{G}_{27}^{(1)3P} = g_0(z) + \epsilon g_1(z) \xrightarrow{z \to 0} -\frac{4}{27} - \frac{106}{81}\epsilon$$

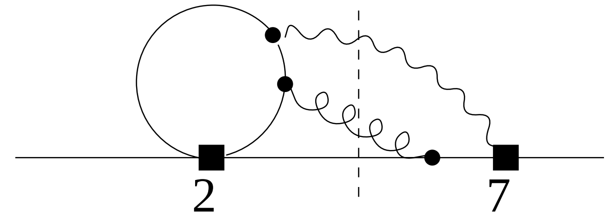

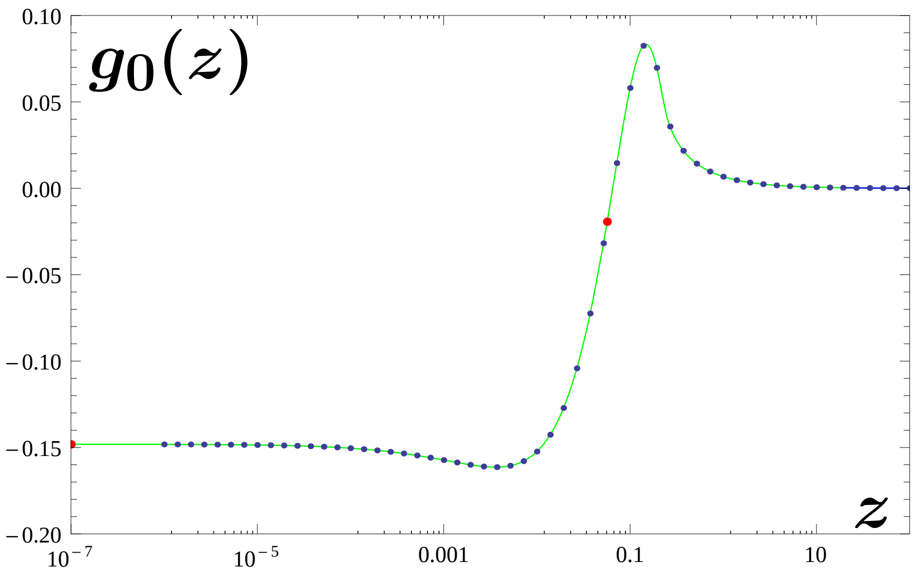

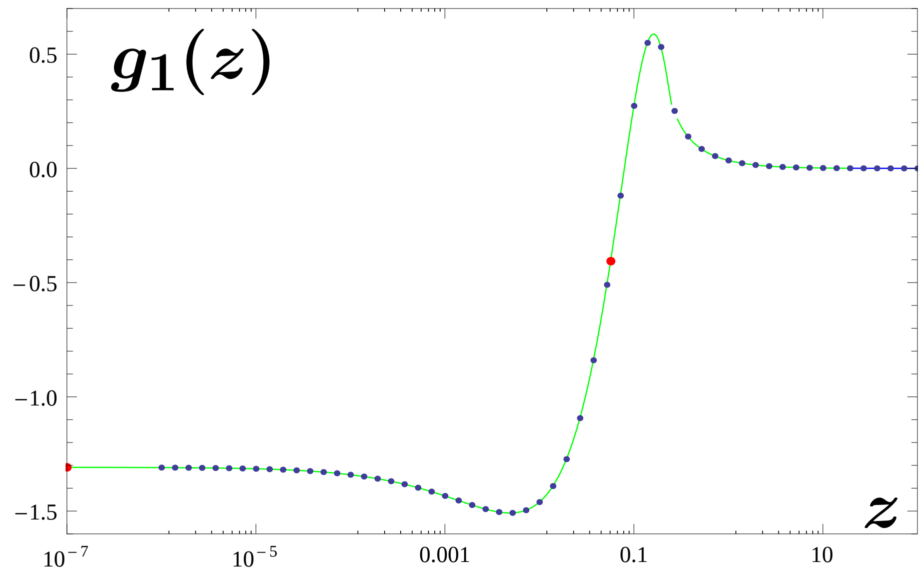

Dots: solutions to the differential equations and/or the exact $z \to 0$ limit.
Lines: exact result for g_0, as well as large- and small-z asymptotic expansions for g_1.

$$g_0(z) = \begin{cases} -\frac{4}{27} - \frac{14}{9}z + \frac{8}{3}z^2 + \frac{8}{3}z(1-2z)\,s\,L + \frac{16}{9}z(6z^2-4z+1)\left(\frac{\pi^2}{4} - L^2\right), & \text{for } z \le \frac{1}{4}, \\ -\frac{4}{27} - \frac{14}{9}z + \frac{8}{3}z^2 + \frac{8}{3}z(1-2z)\,t\,A + \frac{16}{9}z(6z^2-4z+1)\,A^2, & \text{for } z > \frac{1}{4}, \end{cases}$$

where $s = \sqrt{1-4z}$, $L = \ln(1+s) - \frac{1}{2}\ln 4z$, $t = \sqrt{4z-1}$, **and** $A = \arctan(1/t)$.